

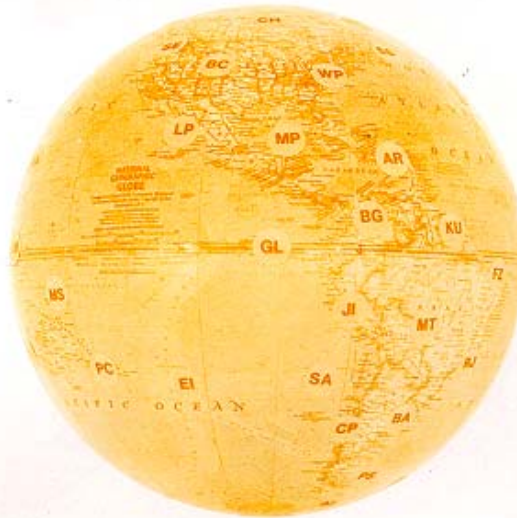


## NOAA SPECIAL REPORT

U.S. DEPARTMENT OF COMMERCE  
NATIONAL OCEANIC AND ATMOSPHERIC ADMINISTRATION  
Environmental Research Laboratory

### Toward Global Monitoring of the Ionosphere in Real Time by a Modern Ionosonde Network: The Geophysical Requirements and Technological Opportunity

J. W. Wright and A. K. Paul



Space  
Environment  
Laboratory

Boulder  
Colorado

July 1981

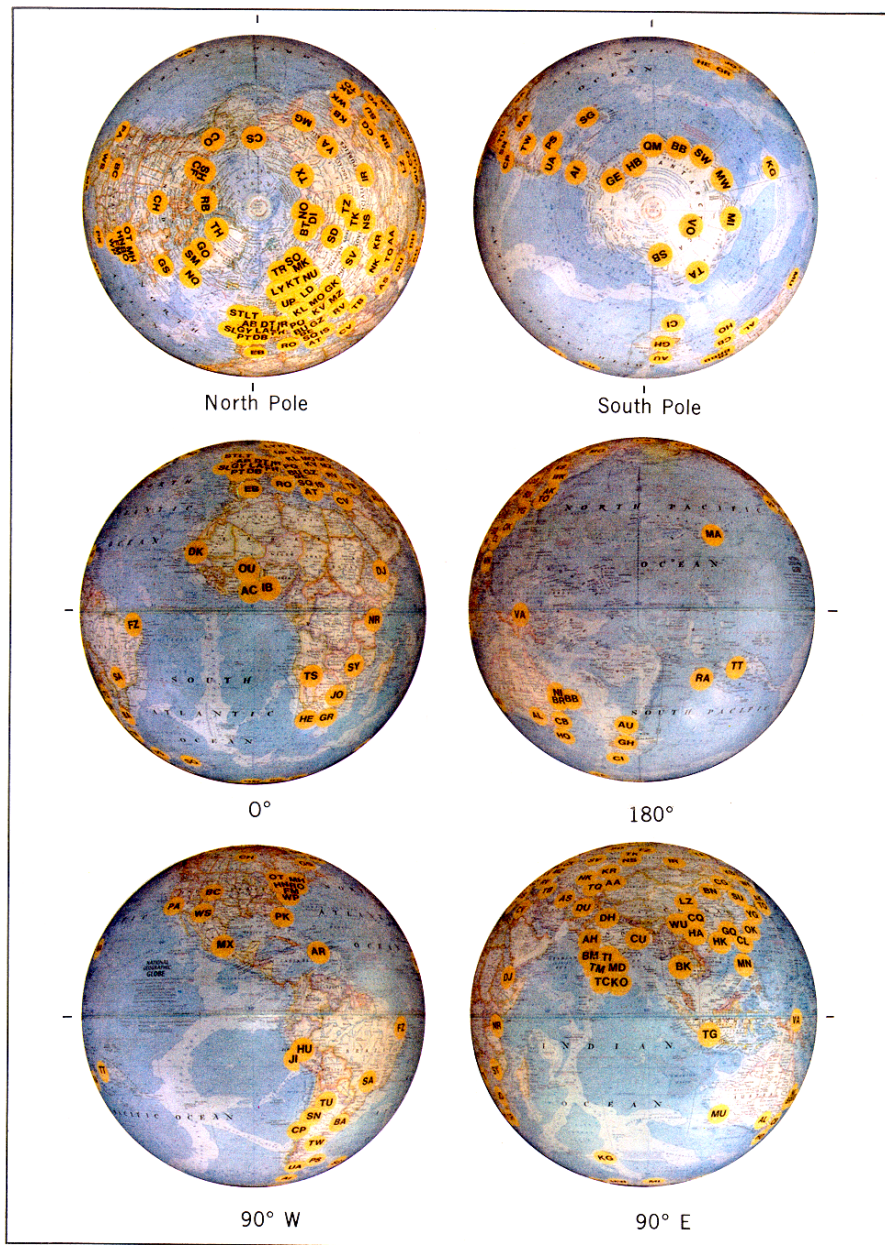


Figure 1. The present active ionosonde network, of about 150 conventional instruments. Stations are listed in Table 2. Station labels have 500-km radius and suggest the field of view afforded by usual antenna systems and instrument sensitivity; however, most conventional ionosondes cannot determine echo location and thus confuse horizontal and vertical structure.

Toward Global Monitoring of the Ionosphere  
in Real Time by a Modern Ionosonde Network

*National Geographic globe [cover and figs. 1 and 15]  
used by permission of the National Geographic Society.*

TOWARD GLOBAL MONITORING OF THE IONOSPHERE  
IN REAL TIME BY A MODERN IONOSONDE NETWORK:  
THE GEOPHYSICAL REQUIREMENTS AND  
TECHNOLOGICAL OPPORTUNITY

J. W. Wright  
A. K. Paul

NOAA Environmental Research Laboratories  
Space Environment Laboratory  
Boulder, Colorado 80303

July 1981



**UNITED STATES  
DEPARTMENT OF COMMERCE**  
**Malcolm Baldrige,  
Secretary**

NATIONAL OCEANIC AND  
ATMOSPHERIC ADMINISTRATION  
James P. Walsh,  
Acting Administrator

Environmental Research  
Laboratories  
Joseph O. Fletcher,  
Acting Director

TOWARD GLOBAL MONITORING OF THE IONOSPHERE IN  
REAL TIME BY A MODERN IONOSONDE NETWORK:  
THE GEOPHYSICAL REQUIREMENTS AND TECHNOLOGICAL OPPORTUNITY

J. W. Wright and A. K. Paul

SUMMARY

We take as granted that improved knowledge of the upper atmosphere is necessary for scientific, social, commercial, and defense purposes; that even as such knowledge advances, practical applications will require continuous monitoring of easily-observable atmospheric properties; that, of these, the concentration of ionization between 60 and 400 km is at once the most informative and easily observable property; and, finally, that HF radio sounding retains an important--and perhaps predominant--role in this field of environmental monitoring.

Current developments in ionospheric sounders demonstrate the advantages of fully computer-interactive systems and digital data acquisition, in which all aspects of system control and real-time data processing are software-defined. Priority is being given to vertical-incidence capabilities, and particularly to automatic estimation of the electron density distribution and its time variation. Two or more such instruments can obtain measurements bistatically to sample ionospheric properties at intermediate locations. Measureable properties, whether by vertical or oblique sounding, include the time and frequency dependence of group path and phase, the signal amplitude, the echo direction of arrival, and polarization. Deducible ionospheric properties again include the vertical electron density distribution, but now extend to its spatial and temporal variations over the region. Reduced data may be exchanged among the systems using the same facilities as used for bistatic soundings. Additional information on ionospheric structure is available to each system by ground backscatter and by passive observation of nearby (100-2000 km) transmitters of known location, frequency, and transmission schedule. Sounder transponders, using telephone lines to return information, can provide additional detail. A global network using ionosonde systems of this kind is virtually certain to evolve naturally out of present interests and capabilities. It will replace the 160-odd obsolete ionosondes now in use with a minimum of about 90 widely-spaced digital ionosonde centers having the capabilities described above, 90 modern instruments being sufficient for global bistatic soundings over 2500-km distances. The natural evolution of this program might consume 25 years, and be rather haphazard. Deliberate planning today can reduce this time and improve the resulting system.

TABLE OF CONTENTS -- FIGURES - TABLES

| <u>Section</u>  | <u>Figures, Tables</u>  | <u>Page</u>        |
|---|---|--------------------|
|   | Fig. 1. Present Network.....                                  | Inside front cover |
| Summary.....  |   | iv                 |
| 1.0 Introduction.....                                     |   | 1                  |
| 1.1 The Present Ionosonde Network.....                    |   | 1                  |
| 1.2 The Role of the Ionosonde in Atmospheric Physics..... |   | 3                  |
|   | Fig. 2. NOAA Dynasonde.....                                   | 8                  |
| 2.0 Dynasonde Measurement Capabilities.....               |   | 9                  |
| 2.1 Hardware Aspects of a Modern Digital Ionosonde.....   |   | 9                  |
|   | Fig. 3. Geophysical Functions.....                            | 10                 |
| 2.2 Geophysical Functions.....                            |   | 11                 |
|   | Fig. 4. F-region Temperatures.....                            | 13                 |
|   | Fig. 5. E-region Collision Freqs.....                         | 14                 |
|   | Fig. 6. F-region Composition.....                             | 15                 |
|   | Fig. 7. E-region Winds.....                                   | 16                 |
| 2.3 The Adaptive N(z,t) Mode.....                         |   | 17                 |
|   | Fig. 8. Automatic Adaptive N(z,t).....                        | 18                 |
| 2.4 The Need for Coordinated Measurements.....            |   | 19                 |
| 3.0 Methods for Lateral Observations.....                 |   | 20                 |
|   | Fig. 9. Coordinated Vertical and Oblique<br>Measurements..... | 21                 |
| 3.1 DYNASND.....  |   | 22                 |
| 3.2 OPORTUNE.....   |   | 24                 |
| 3.3 BAKSCTR.....  |   | 25                 |
| 3.4 BISTAT.....   |   | 26                 |
| 3.5 TRNSPND.....  |   | 27                 |
| 4.0 Considerations Affecting Network Deployment.....      |   | 28                 |
| 4.1 Idealizations.....                                    |   | 28                 |
|   | Fig. 10. Idealized Dynasonde Distribution.....                | 28                 |

|     |   |                   |
|-----|---|-------------------|
| 4.2 | The Geophysical Requirements.....                             | 30                |
|     | Fig. 11. Correlation Distance of foF2.....                    | 31                |
|     | Fig. 12. AFA (foF2) Constant Component.....                   | 32                |
|     | Fig. 13. AFA (foF2) Diurnal Component.....                    | 32                |
| 4.3 | New Standard Parameter Products from a<br>Modern Network..... | 33                |
|     | Fig. 14. Present and Proposed Parameters.....                 | 34                |
| 4.4 | Volume of Information From a Modern Network.....              | 38                |
|     | 4.4.1 Data Volume From the Present Network.....               | 39                |
|     | 4.4.2 Data Volume From a Modern Network.....                  | 40                |
| 4.5 | Further Data Assimilation at Regional Centers.....            | 43                |
|     | 4.5.1 Month by Hour Summaries.....                            | 43                |
|     | 4.5.2 Regional Mapping of Mean Values.....                    | 44                |
|     | 4.5.3 Global Mapping of Mean Values.....                      | 45                |
|     | 4.5.4 Mapping of Spectral Components.....                     | 45                |
| 5.0 | The Deployment of a Practical Modern Network.....             | 46                |
|     | Table 1. Gaps in Global Coverage.....                         | 47                |
|     | Table 2. Current and Suggested Stations.....                  | 48                |
| 6.0 | Conclusions.....  | 51                |
|     | References.....   | 57                |
|     | Fig. 15. A Suggested Modern<br>Network.....                   | Inside back cover |

TOWARD GLOBAL MONITORING OF THE IONOSPHERE IN  
REAL TIME BY A MODERN IONOSONDE NETWORK:  
THE GEOPHYSICAL REQUIREMENTS AND TECHNOLOGICAL OPPORTUNITY

J. W. Wright and A. K. Paul

1.0 INTRODUCTION

1.1 The Present Ionosonde Network

There are about 160 ionosondes operating on the globe today (Figure 1), at locations discussed in Sect. 5. Only a handful of these are reasonably modern instruments, the great majority following design concepts developed in the 1940's and 1950's. They commit their measurement information to analog film in the form of ionograms. Even a few manually tuned instruments are still in regular use, requiring full-time operators. Only a small fraction (usually 25%) of the ionograms are reduced to numerical data. Reckoned in terms of directly meaningful geophysical quantities this amounts to some half-dozen parameters manually digitized for each hour. Long multi-solar-cycle time series of only a few of these parameters are available and from only a few stations. Conversion of ionograms to electron density profiles,  $N(z)$ , is done only irregularly, with a few exceptions (Wright and Smith, 1967; UAG-54, 1976, p. 27-29).

This is an unnecessarily wasteful situation, and it should not be continued through the 1980's. Many of the present installations (Figure 1) should be considered by their governing administrations, not as better-than-nothing contributions to an international network, but as actual and active obstacles to the



evolution of a serviceable network. An unfortunately prevalent example of the counterproductivity of the traditional methods is their preservation (usually under government sponsorship) at educational institutions. This becomes more evident when the modern alternatives are understood. Despite the immediate impression which this paragraph might give, it is not intended as an incentive to the abrupt and arbitrary termination of ionosonde stations. Instead, we wish to encourage a planned redistribution of the present resources, leading to a smaller number of modern stations that, individually and collectively, will provide much more information (and do so more rapidly) than the present network.

It must be emphasized that the stations of Figure 1 function in a largely uncoordinated manner; it is usually only in a long-term (monthly-median) sense that this degree of global coverage can even be approached. To a contrasting extreme, Europe, parts of the Soviet Union, India, and the Far East are saturated with traditional instruments. Several regional programs (USA, USSR, France, India) represent and forecast large-scale ionospheric structure, e.g., Argo and Rothmuller (1979); Hatfield (1979). A global program (Thomson and Secan, 1979) is maintained by the AFGWC, based in part upon data from 44 widely-spaced ionosondes (some providing near-real-time parameters). However, this comparatively ambitious effort is considered data-starved by its authors.

Apart from such needs for more data, is there a need for a modern alternative? We feel that this question is too easily

evaded by the demonstration that only a fraction of the information obtained from the present network is actually used. (What is demonstrated, of course, is that most of this information is not useable.) The practical need for a modern ionospheric monitoring network is best presented by those who would or could use the information in telecommunication, environmental, defense, and commercial applications (Rush, 1976). As geophysicists, we can assert with confidence that data from a modern network will certainly be used in geophysics. The data will be in computer-accessible form and expressed in geophysical parameters, at the point of measurement. Although the geophysical community probably cannot bring about a modern network for its goals alone, we believe that these goals serve, and subsume, those of all the others.

#### 1.2 The Role of the Ionosonde in Atmospheric Physics

"The ionosphere occupies a key position in solar terrestrial physics because, extending up to the magnetosphere and down to the domain of meteorology, it impinges on both" (Rishbeth and Kohl, 1976). Analogously, radio sounding by total reflection occupies a key position in ionospheric measurement: the plasma is a sensitive tracer of virtually all atmospheric processes underway in the ionosphere, and radio wave reflection provides a plasma probe of unparalleled sensitivity. High signal-to-noise ratios are obtained easily with systems of modest power and without recourse to compromisingly long signal integration times. Radio frequency gives electron density directly at total reflection, and distances are measurable to about 1% of the radio

wavelength, a few meters. Some of the measurements are useful directly, without conversion to geophysical parameters, as in the representation of long-distance radio communication conditions. They may also be inverted to a variety of atmospheric information, much of it available in no other practical way. The methods can provide information on all temporal scales, extending from the beginning of our awareness of the ionosphere a half-century ago, down through those (of solar or terrestrial origin) occupying fractions of a second. Information describing a wide range of spatial scales is accessible from a single observing location, typically starting with those comparable to the radio wavelengths used (.01-.3 km) and extending far beyond the first Fresnel zone scale (typically 3 km) to horizontal scales at least as large as the height of the ionosphere (100-300 km).

These features are not obtained without some compromise, of course. Total reflection itself means that the topside ionosphere (and, occasionally, everything above an intense sporadic E layer) is beyond observation. It has been historically more significant that for purposes other than simple radio propagation applications, the wanted geophysical information is only indirectly available from total reflection measurements. Numerical inversion procedures, some of them rather difficult or uncertain, are usually required. To attain the full benefit of total reflection sounding under these circumstances, there are three inescapable requirements:

- (1) The measurement system must have complete agility in time and frequency sounding patterns, and it must obtain a full description of each radio echo. This has only recently become possible, and it follows that the system must be programmable and digital.
- (2) The measurements must be fully reduced to the geophysical information they contain; otherwise, when reduction is incomplete, the interpretation of each part suffers unnecessary ambiguity.
- (3) Global (or at least regional) and continuous monitoring is necessary; first for obvious reasons identical to those for meteorology, and also--as suggested by this paper--for the temporal and spatial continuity of measurement that provides the necessary information by which each instrument can adapt its data acquisition pattern to prevailing conditions in the ionosphere.

In the following sections we summarize the demonstrated measurement capabilities of the "Dynasonde" class of ionospheric measurement systems (Wright, 1969; Wright and Pitteway, 1979 a,b), that we believe satisfy requirement (1), above. We also describe some natural extensions of these capabilities to provide oblique incidence, backscatter, and passive observations of the ionosphere, each contributing to increased lateral coverage. Examples of available data processing procedures are given to illustrate the present position with regard to requirement (2); we also identify some further developments which

are needed. Finally, we attempt to suggest the size, deployment, modes of operation, costs, and benefits of a global ionospheric monitoring network satisfying requirement (3).

Two additional introductory comments seem worthwhile. First, it is frequently proposed that ionospheric predictions and morphology can be derived (eventually, at least, and to some useful approximation) from theoretical modeling, instead of from empirical observation. Without wishing to risk judgment of this question for the distant future, we suggest that at present this view inverts the role that theoretical models can and should play. Furthermore, this view purports to conclude that an ionospheric monitoring network is not needed. Again, the analogy with meteorology is instructive. Ionospheric weather is immediately and easily observable by radio sounding, and the problems of short-term predictions (i.e., projection) and morphology can be reduced to those of data processing and communications, if an adequate observing program is maintained. The proper use of theoretical modeling, we feel, is to extract from empirical observation of the ionosphere those properties of the atmosphere that are difficult to observe directly. We suggest some examples later.

Second, we wish to emphasize the close relationship to be anticipated between monitoring and research should a network of modern ionosondes be established. The research worker requires background (or monitoring) data in nearly every investigation, and most observational research programs can augment the monitoring data base. An important feature of the Dynasonde class of

digital ionosondes is its ability (through suitably programmed operating systems) to maintain scheduled monitoring activities while performing research-oriented measurements as well. Further significant improvements in the practical applications of ionospheric knowledge (e.g., for communications, environmental concerns, detection of unnatural disturbances, etc.) is surely to be gained through improved understanding. And improved understanding demands the more comprehensive monitoring effort proposed here.

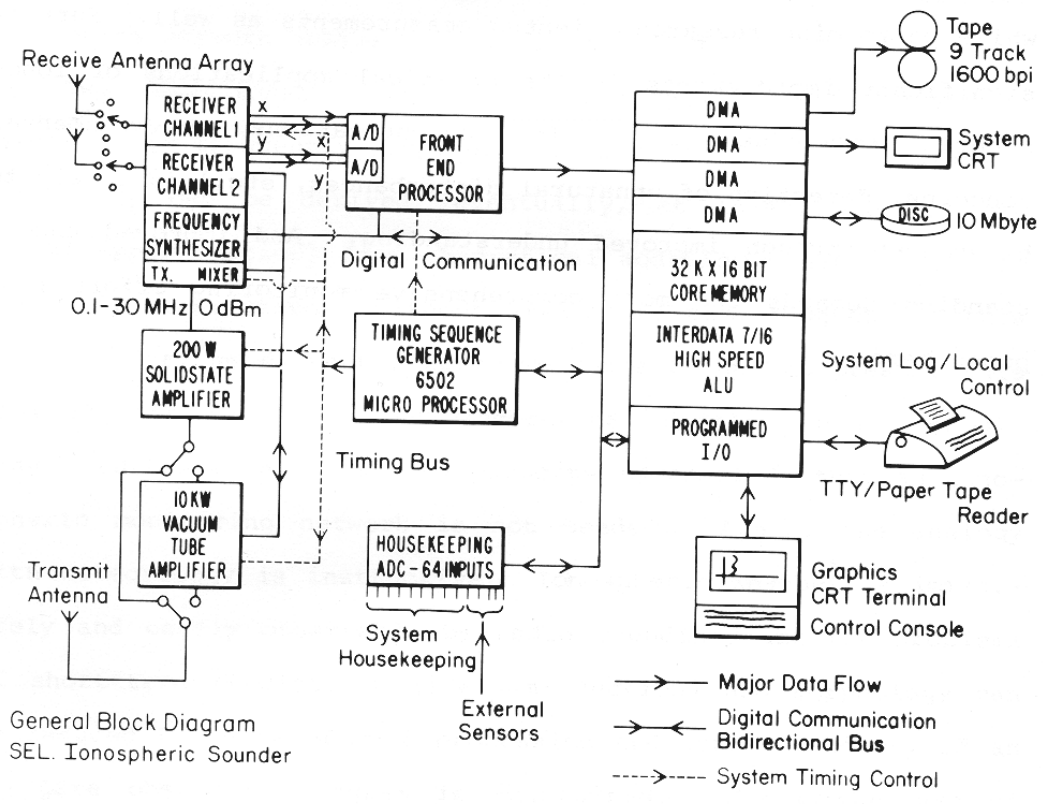


Figure 2. Functional and hardware layout of the digital ionosonde currently assembled at NOAA, Space Environment Laboratory. Note the microprocessors dedicated to system timing and to real-time digital signal processing from two parallel quadrature receivers. Full system control for data acquisition, data processing, and user interaction is achieved through software in the general-purpose minicomputer.

## 2.0 DYNASONDE MEASUREMENT CAPABILITIES

### 2.1 Hardware Aspects of a Modern Digital Ionosonde

The necessary hardware features of Dynasonde systems have been adequately described elsewhere (Wright, 1975a, 1977) and need not be reviewed here. It is sufficient to show, with Figure 2, the functional layout of the latest such system as designed and assembled at NOAA-SEL by R. N. Grubb. The general-purpose computer, supported by the usual digital peripherals and by two microcomputers dedicated respectively to real-time signal processing and system timing management, are the essential features by which requirement (1) of our Introduction is achieved. The minicomputer, disk memory, and tape provide a large potential for real-time and deferred data processing, in addition to complete flexibility for defining data acquisition patterns. Realization of the full potential of these instruments will require a considerable amount of further software development and field tests. However, much of this potential has been demonstrated in a prototype Dynasonde (Wright, 1969, 1975a,b, 1977; Wright and Pitteway, 1979a,b). Much more on the matter of oblique incidence radio measurements has been accomplished elsewhere quite independently of the Dynasonde, but these methods may be incorporated into the new instruments through software (and perhaps some hardware) extensions. (See, for example, Barry and Fenwick (1969), Hatfield (1970), Smith (1970), Chernov (1971), Croft (1972), Nielsen and Watt (1972), Rao et al. (1976), Dubroff et al. (1978), Miller and Gibbs (1980).)



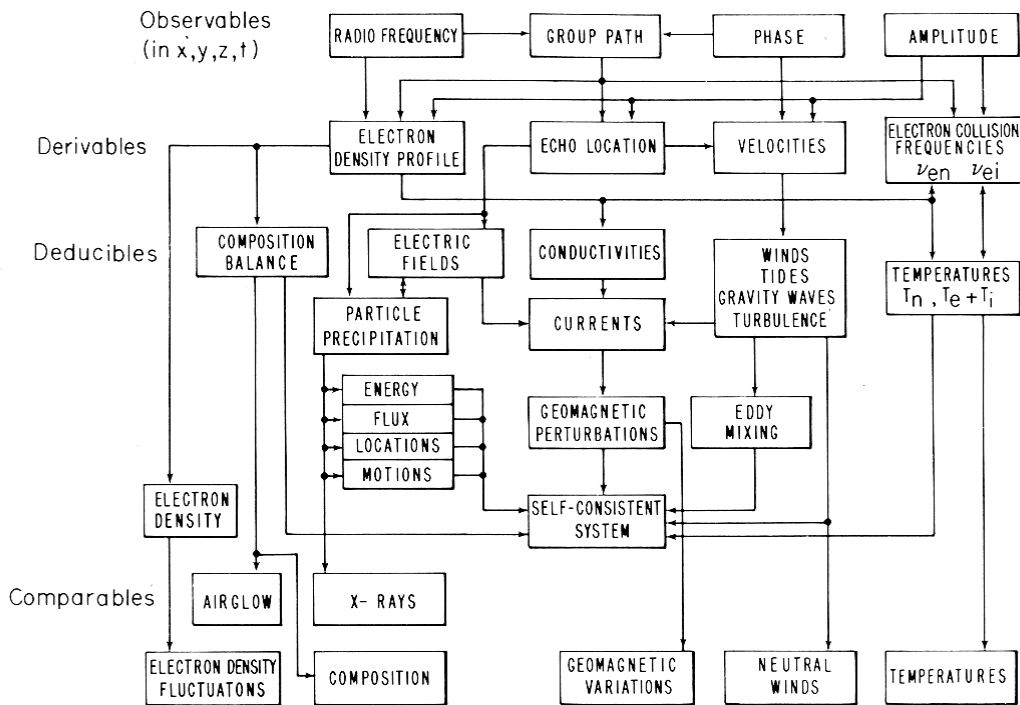


Figure 3. Geophysical functions of a digital ionosonde, showing relationships among the measurable quantities (observables) in ionospheric total-reflection radio sounding, and the geophysical properties of the ionosphere and atmosphere. Note the interdependence of the derivable and deducible properties on all of the observables.

## 2.2 Geophysical Functions

Figure 3 suggests four geophysical functions of a digital ionosonde:

Observables are the dependent variables which are measured for each ionospheric echo--effectively the group path and phase, and echo amplitude. These (or equivalent) quantities must be obtained as functions of the independent variables for space, time, and radio frequency. The frequency converts directly to plasma density, but the spatial localization of the echo is an involved inversion problem.

Derivables are quantities obtained by calculation from the observables using established theory and (if appropriate) statistically informative estimation procedures. The status of some of these data inversion procedures was discussed by Wright (1975a). They include methods for obtaining the electron density distribution from multifrequency vertical, oblique, and backscatter soundings; methods for locating and tracking discrete targets of medium scale; and methods for deriving ionospheric velocities.

Deducibles are almost all of the parameters, properties, and processes of the higher neutral atmosphere and ionosphere. Some of these (e.g., winds, conductivity) are almost directly related to observables and might be included in the derivable category. Others (e.g., eddy mixing, electric fields) are hardly observable by any direct means and must be deduced from their effects.

Comparables are quantities or processes that are measurable by means entirely independent of radio sounding. They are often important for validation of data acquisition and inversion methods, and the ionosonde may offer as much, if not more than it receives, in such comparisons.

A few examples are worthwhile to support some of the deducibles of Figure 3 that are less widely recognized as available by total-reflection sounding.

Ionospheric Temperatures: The plasma temperature (the mean of the electron, ion temperature) controls the F2 layer thickness apart from transient departures due to winds, waves, and electric fields. The scale height and plasma temperature are thus available (after averaging away transitoria) from the curvature of the N(z) profile at the layer peak (Rishbeth and Garriott, 1969, 4.41). That this works in practice is suggested by a number of synoptic studies (Wright, 1963, 1964; Becker and Stubbe, 1963; Rohrbaugh et al., 1973) and by the small sample of direct-comparison data in Figure 4.

An entirely independent method for obtaining temperatures is based upon the deviative absorption suffered by radio waves reflected near E and F layer peaks (Ganguly, 1974; Saha and Venkatachari, 1975). An example (from Danilkin et al., 1978) is shown in Figure 5; it compares values of collision frequency made near the E peak (96-110 km) with values computed using gas-kinetic theory and an atmospheric model. The collision frequency and (neutral) temperature are closely related at E region

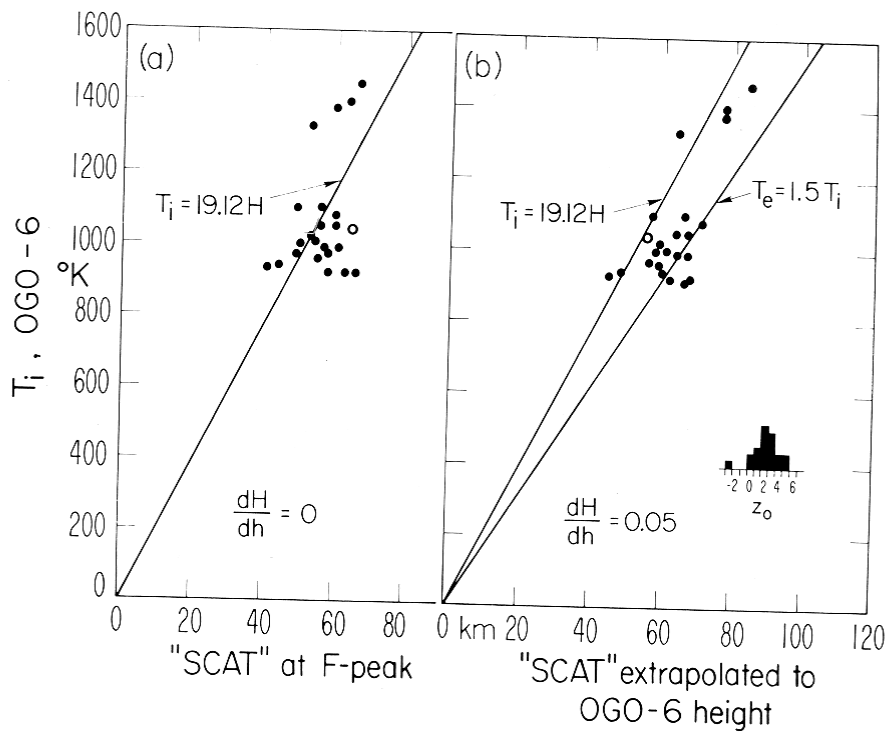


Figure 4. Measurements of ion temperature at satellite altitude (0-5 scale heights from  $h_{\text{max}}\text{F2}$ , as shown by the  $Z_0$  insert) from a small sample of OGO-6 satellite passes over ionosonde stations, compared with the curvature (expressed as a scale height) at the F2 layer peak from ionosonde  $N(z)$  profiles. Right and left panels show the effects of unequal  $T_e$ ,  $T_i$  and of a temperature height gradient.

altitudes, but comparative data are desirable to validate the deduction of temperature.

Neutral Composition: The F2 layer electron density depends strongly on the composition ratio  $[O]/[N_2]$ , and several authors have used this to deduce the ratio (and related neutral composition information) from  $N(z)$  profiles (Prölss et al., 1975; Antoniadis, 1976). The example of Figure 6 (from Stubbe, 1973)

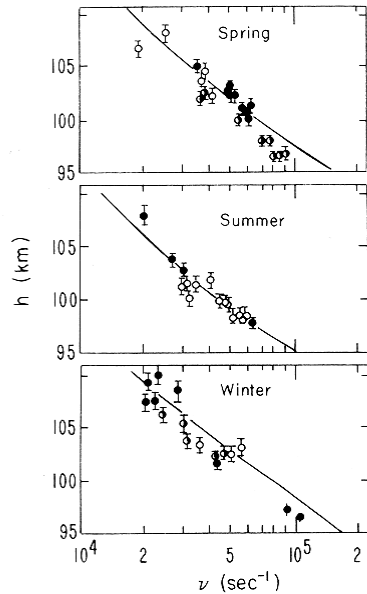


Figure 5. Height variations of electron collision frequency near the E-layer peak deduced from radio wave deviative absorption (plotted points) compared with gas-kinetic calculations using an atmospheric model (from Danilkin et al., 1978).

compares composition ratios from the curvature of the  $N(z)$  profile the layer peak with measurements by the OG0-6 satellite and by 6300-Å airglow. The practical use of such deductions may certainly be questioned, at least until more calibration and modeling have been carried out, but these examples show the proper role of theoretical modeling and the importance of identifying self-consistency in the system illustrated by Figure 3.

Neutral Winds: It is now well-established that analysis of the moving radio diffraction pattern, measured at the ground, yields a good estimate of the neutral air motion at the radio reflection level in the E region (Figure 7; Wright et al., 1975 a,b). This makes the measurement of winds virtually direct and derivable, although the statistical analysis procedure is rather lengthy (Fedor, 1967). [A simplified procedure has been developed by

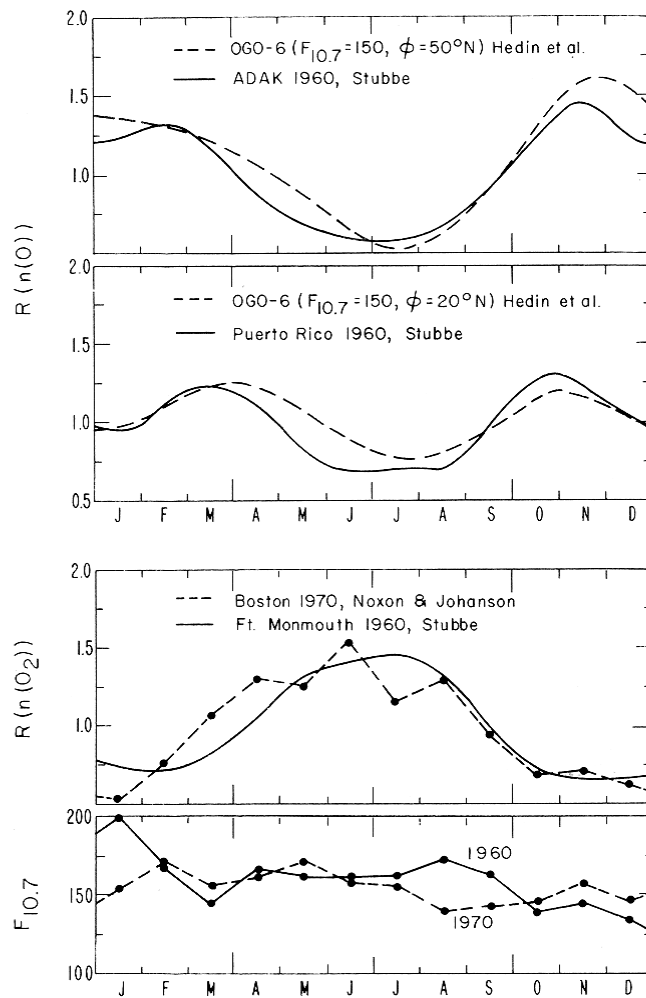


Figure 6. Relative seasonal variations of O density from ionograms (Stubbe, 1973) and from OGO-6 (Hedin et al., 1972); of  $O_2$  density from ionograms (Stubbe, 1973) and from 6300A airglow (Noxon and Johanson, 1972).

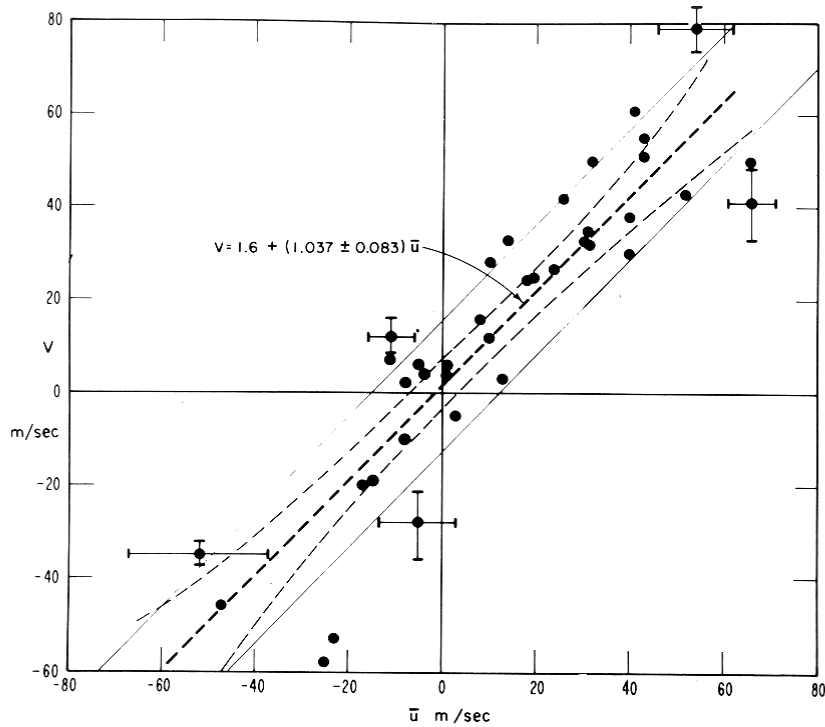


Figure 7. The close experimental relationship between  $V$ , the radio spaced-antenna moving-pattern mean velocity, and  $u$ , the mean meteor-radar wind velocity. Correlation coefficient (39 cases) is 0.912. Each value pair represents 4 min of "kinesonde" measurement at one altitude, between 92 and 103 km, compared with 8-28 individual meteor winds measured near the same time ( $\pm 50$  min, typically) and near the same altitude ( $\pm 2$  km, typically) (from Wright et al., 1975a).

Paul (1977, unpublished) for real-time use in a digital ionosonde and is being tested.] The reason that radio diffraction from the plasma can convey information on the neutral air motion, even when the bulk motions of the two gases may differ, is not fully understood; presumably, irregularities in the two gases are closely coupled even where their motions are not.

Numerous other examples of parameters and phenomena deducible from ionospheric radio sounding may be mentioned:

Substorm electric fields (Ruster, 1965)  
Energetic particle precipitation (Wright, 1975b)  
Large-scale atmospheric waves (Thome, 1964;  
Morgan et al., 1978; Harper and Bowhill, 1974)  
Jet-stream induced waves (Vidal-Madjar et al., 1978)  
Tsunami-warning (Najita et al., 1974)  
Atmospheric explosions (Broche, 1977)  
Aircraft-induced disturbances (Marcos, 1966)

### 2.3 The Adaptive N(z,t) Mode

By far the most fundamental item of information to be derived from radio sounding is the electron density profile,  $N(z)$ . An automatic procedure that optimizes input data selection has been demonstrated (Wright et al., 1972), and a simplified but accurate inversion routine for minicomputers is available (Paul, 1977). Awaiting further development in the new digital ionosondes is the adaptive real-time profile measurement system (A-mode) illustrated in Figure 8 for  $N(z,t)$ . Although there may be about 1000 measurement frequencies in a typical ionogram, less than 50 of these are usually selected (subjectively) for group-range input to the inversion procedure. The AUTONH process automates and optimizes this selection, on the basis of knowledge of the preceding profile. The adaptive procedure of Figure 8 uses the specification of optimum frequencies, in a further step, to control the sounding activity itself. By thus separating the functions of ionogram sounding (which is still useful for its familiar display of ionospheric structure) from the  $N(z,t)$  profile function, much better temporal resolution and continuity



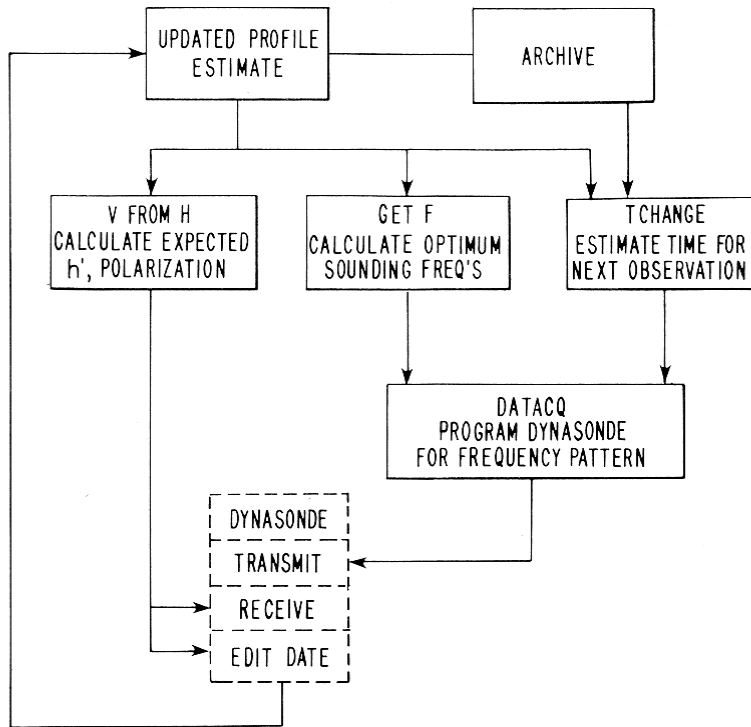


Figure 8. Automatic, adaptive  $N(z,t)$  inversion. A profile estimate,  $N(z)$ , is used by GETF to decide the optimum sounding frequencies; VFROMH predicts the expected group heights. DATAQ programs the Dynasonde to observe updated  $R'(f)$ , from which the next profile  $N(z)$  is computed. Meanwhile, TCHANGE monitors the time rate of change of profile parameters to influence the sounding schedule.

may be achieved in the profile. Furthermore, it seems reasonable that the same frequencies as are selected dynamically in A-mode (plus a few others to make the procedure more robust) are also the optimum frequencies for drift, angle-of-arrival, temperature, and other estimation procedures.

#### 2.4 The Need for Coordinated Measurements

Returning our attention now to Figure 3, we observe two similar points that deserve separate emphasis, each of which involves the lines among boxes in that diagram rather than the boxes themselves:

First, the relationships among derivable and deducible properties are identical to the subject matter often termed theoretical modeling of the ionosphere and high atmosphere. Although particular links between boxes must often be developed in isolation, it is the degree of success of the entire pattern as a self-consistent system that expresses our state of knowledge. If important links are omitted in the modeling, or are inaccessible because of measurement system limitations, confidence in the entire structure suffers. An important advantage of HF sounding is that it can stand alone, if necessary, in providing the essential input to most of Figure 3.

Second, specifically regarding total reflection sounding, we must emphasize the interdependent character of the observables in their relation to the derivables. Earlier sounding systems that, for example, measured ionospheric absorption, Doppler, direction-of-arrival, or drifts, at one frequency only, were exploratory and developmental efforts of pioneering value. However, it is

only through doing all of these in concert that the modern digital ionosonde can be expected to perform adequately for the geophysical functions of Figure 3.

An extrapolation of this second point provides the main theme for the present paper. A very small number of digital ionosondes, however sophisticated, can not satisfy requirements for global monitoring of propagation, ionospheric, or geophysical conditions, but a threshold exists at which a moderate number of competent instruments, operating with real-time coordination, can do so. In addition to the vertical-incidence measurement capabilities just described, it is possible to use the same hardware and data processing facilities with relatively little modification for measurement of lateral variability in the ionosphere.

### 3.0 METHODS FOR LATERAL OBSERVATIONS

Ionosondes with typical power, sensitivity, and antenna systems have a field of view roughly comparable with the radius of the station labels in Figure 1, that is, about 500 km for the F region and proportionately less for the lower ionosphere. A horizontal component of the local ionization gradient displaces the condition for total reflection from overhead, and variations of the gradient, if large enough, can cause multiple specular points to occur. These are abundant and self-evident in routine ionograms, but in such recordings, lacking any information concerning echo direction of arrival, the lateral and vertical structure is usually confounded. This is another example of the

counterproductivity of the standard ionosonde.

In modern instruments (Figure 1) accurate measurement of echo complex amplitude at a closely-spaced array of receiving antennas permits calculation of the direction-of-arrival of each echo (Paul et al., 1974; Wright and Pitteway, 1979b). If, in addition to the vertical-incidence transmitting antennas, there are available broad-band antennas producing low-elevation radiation in several azimuths, the same ionosonde can obtain a much greater lateral view by a variety of well-established or potentially valuable methods. Figure 9 suggests the relationships among these methods, and gives pseudo-acronyms for the sake of brevity in identification.

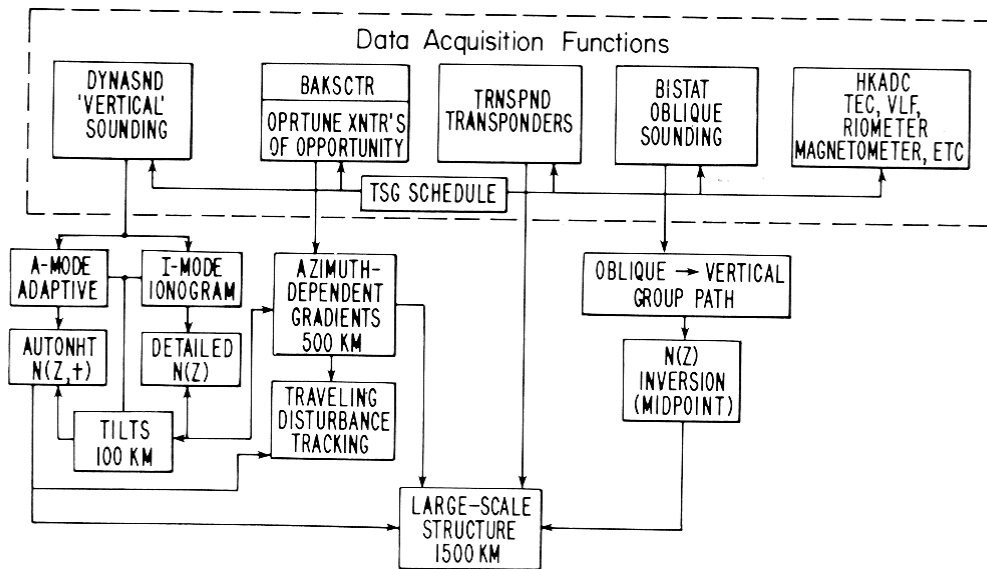


Figure 9. Coordinated vertical and oblique measurements showing relationships among the principal data acquisition modes of the Dynasonde, and the data processing methods needed to support and interpret the measurements.

### 3.1 DYNASND

Measurement of the zenith and azimuth angles-of-arrival during ionogram or adaptive soundings provides information on the nature and magnitude of ionosphere tilts and horizontal gradients. If the tilt changes slowly with radio frequency (height) or time, a large-scale structure is implied; small-scale structures produce correspondingly smaller time and height scales. Qualitatively different effects occur for intense structure of small-scale: more than one normal-incidence reflection point may occur, and looping ray paths (not involving normal incidence) are found occasionally (Paul et al., 1968). Doppler information may provide an extra dimension of discrimination when multiple ray paths are known or suspected (Pfister, 1971; Brownlie et al., 1973).

Methods for converting this lateral information into a quantitative three-dimensional description of the local ionosphere are not well developed. Distinct targets (e.g., Cs<sup>+</sup> clouds, Wright, 1974) can be located and tracked by echolocation calculations from spaced antenna data, and the same techniques are clearly applicable to electron clouds produced by energetic particle precipitation and to other discrete sporadic E patches. Irregularities with soft boundaries embedded in the higher ionosphere are more difficult to observe and to interpret. They must be divided according to whether their electron density exceeds the background density or is exceeded by it. Depletions tend to be more observable than ionization enhancements since the far side of a hole provides a concave focusing surface. Con-

versely, enhancements create defocusing surfaces, and unless these are below about 150 km altitude (where small-scale irregularities give them a rough scattering surface) they may escape detection by ionosondes (Wright and Paul, unpublished manuscript describing Ba<sup>+</sup> cloud experiments at various altitudes). Even when abundant echoes from an embedded disturbance are available, no direct inversion procedure is available to convert the data to a description of the irregularity. Iterative ray-tracing is necessary to simulate distinctive properties of the data such as group range, angle-of-arrival, frequency-dependence, observing location (Paul et al., 1968). For much larger gradient scale lengths, a method is needed to combine electron density profile inversion with echo-location. A first-order correction for layer tilts is easy: the echo-location calculation yields the group path vector (Paul et al., 1974), and the vertical component of the vector can simply be used for h' in the profile inversion. While this approach may somewhat improve the profile estimates (in the sense of yielding profiles that are more consistently vertical) it is only an approximation, and it yields little direct information on the lateral gradients except when the large scale of a tilt is self-evident. The analysis can be carried further by ray tracing at the measured angle-of-arrival into the vertical profile introducing enough tilt to obtain normal incidence reflection at the critical ionization contour. This procedure is suggested in Figure 9. The analysis then requires iteration. These methods can be expected to provide an acceptably accurate description of lateral variability within a 100-km radius.

### 3.2 OPORTUNE

Passive observations of "transmitters of opportunity" might provide useful supplementary information concerning lateral gradients and traveling disturbances, at the cost of data processing only. For remote transmitters of known schedule, location, and frequency stability, the digital ionosonde can measure the presence, field strength, Doppler, and angle-of-arrival of the signal. A minimum of about 0.5-sec observation per frequency should be sufficient for this, divided equally between the same two orthogonal pairs of receiving antennas that are used for vertical sounding. However, it should be noted that Baulch and Butcher (1978), who performed CW angle-of-arrival experiments of this kind, suggest that much longer observation times (10 sec) are desirable to reduce effects of mixed 1-,2-hop signals. OPORTUNE might be applied to signals originating out to the 1-hop limit (2000-4000 km) in principle, but, since this implies low arrival angles, short wavelengths, and vertical polarization, special antennas would be needed. It is probably better to advocate the method for shorter distances, say between 200- and 1000-km ground range, until its usefulness and limitations are better established. If, in each of six azimuths, five transmitters at ranges of about 200, 400, 600, 800, and 1000 km were available, OPORTUNE would require 15 seconds for data acquisition. The sampling of each azimuth should be followed by its 180° complement since the information from such paired directions is most easily combined with the vertical sounding results.

### 3.3 BAKSCTR

With transmitting antennas that favor a particular azimuth and an intermediate zenith angle, oblique backscatter at frequencies exceeding the overhead critical frequency may be observed. About all that is seen by systems of ordinary power is the so-called leading-edge backscatter, the envelope of skip-distance or minimum-time-delay scatter, and even that is seldom available beyond half-paths of about 1500 km. Within the observable range, however, the trace provides nearly direct information on the variation of maximum density with distance from the observing location. Computer simulation and the development of backscatter data analysis is being pursued actively by the University of Illinois (DuBroff et al., 1978); backscatter measurements have been used to map foF2 within a radius of 1500 km, by Hatfield (1970). The analysis is again iterative; starting from the local vertical distribution, it attempts to match group-range by ray tracing in a model with adjustable gradients of peak density, height, and thickness. DuBroff et al. (1978) show that these parameters can be recovered with acceptable accuracy from the data. However, the methods require considerable computer time, even in a large machine, and uniqueness suffers in the presence of quadratic gradients and underlying ionization.

For tracking sporadic E clouds these refraction problems do not arise, and backscatter can be a powerful tool for detecting such clouds and for estimating their diameters, velocities, and sizes (Tanaka, 1979).



### 3.4 BISTAT

Bistatic oblique sounding over 1-hop paths provides a means for probing the ionosphere at the path midpoint. If transmission and reception in both directions is performed, the absolute group-path delay is the mean value of the two observed echo delays measured from the local transmission times. The only timing accuracy required is that which is sufficient to assure frequency synchronization and is of the order of the repetition interval. Numerous experimental programs of oblique sounding have been carried out (Davies, 1965, §4.41), and some specific propagation paths are routinely monitored by the chirp version of the hardware (Barry and Fenwick, 1969). Inversion of oblique ionograms to midpoint  $N(z)$  profiles is not fundamentally different from the vertical sounding problems (Chuang and Yeh, 1977), but some quantitative distinctions are important:

- (1) For the same electron density at reflection, a higher radio frequency is required in proportion to the secant of the take-off zenith angle.
- (2) Magnetoionic effects, important for separate consideration of ordinary and extraordinary propagation modes at vertical incidence, become steadily less important as the distance of oblique propagation increases. Partly, this results from the use of higher frequencies in relation to the electron gyrofrequency. But more important is the averaging effect of the larger scattering region that tends to blur the  $O/X$  resolution in

the measurements (Barry and Fenwick, 1969); since O and X are affected oppositely--if not equally--from the no-field case, neglect of the magnetic field (in ray tracing, for example) offers a valuable simplification.

- (3) Screening of a higher part of the ionosphere by a lower part (or by the horizon itself) can be troublesome for profile inversion. The problem is similar to valley or sporadic E blanketing in the vertical-incidence case, but can be more prevalent at oblique incidence because the layer density and height effects are combined in determining the screening height.
- (4) Horizontal gradients may cause significant displacements of the reflection points from the path midpoint, especially for the longer 1-hop paths contemplated here. It is not known whether measurements of angle-of-arrival will provide useful additional information for estimating these gradients.

### 3.5 TRNSPND

Simplified systems (receive and digitize only) can be located at distances of 50-500 km from each ionosonde location, on various azimuths--geography permitting. These could provide higher spatial resolution in certain regions.

#### 4.0 CONSIDERATIONS AFFECTING NETWORK DEPLOYMENT

##### 4.1 Idealizations

A purely geometric approach to station deployment, while obviously impractical to realize, provides a few useful insights (Figure 10). The ratio of the Earth's surface area (radius R) to that observable from a single site (radius r) is  $4 R^2/r^2$ . If r is taken to be 1000 km, 162 sites are required; 113 for

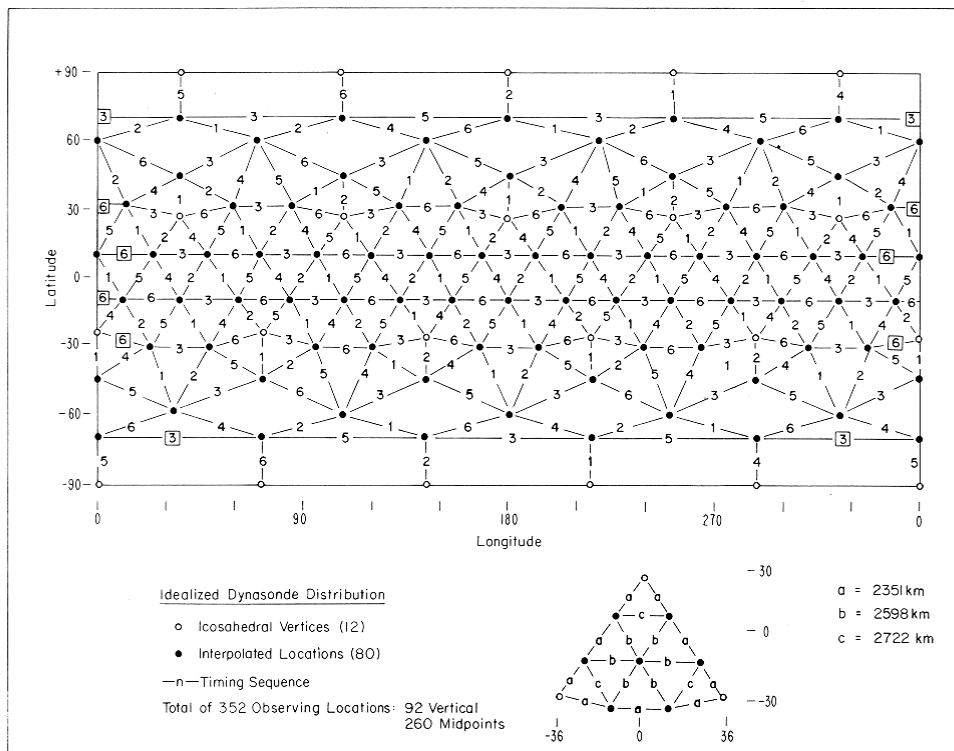


Figure 10. An idealized station deployment based upon the twelve vertices of an icosahedron (o), each of the 20 faces of which are further divided (●) into nine nearly equal isosceles triangles. Small numbers between sites suggest a possible schedule of bistatic soundings between adjacent station pairs in a cycle of six.

$r = 1200$  km; and 72 for  $r = 1500$  km. On the other hand, the Platonic solids provide relationships among the number of vertices, edges meeting at vertices, etc. The maximum possible number of equidistant vertices touching the surface of a sphere is 20 (the dodecahedron), but only three edges (directions for bistatic sounding) meet at each vertex, and obviously the interstation distances are far too great for 1-hop propagation. The icosahedron (12 vertices) affords six equidistant directions, which seems ideal, but the distances are still greater.

A satisfactory plan may be based upon the icosahedron by dividing each edge by three and adding one vertex near the center of each equilateral face. This produces isosceles triangles in each face, as shown by the sketch at lower right in Figure 10. If the Earth were divided in this way, 92 station locations would result, with three characteristic interstation distances: 2351, 2598, and 2722 km. These distances are all comfortable for bistatic oblique sounding of the F region. In addition to the 92 observation sites for vertical observations, the contiguous-pair midpoints provide 260 additional measurement locations. Each of the 12 icosahedral vertices "sees" five interpolated sites at equal azimuths of  $72^\circ$ , while each of the interpolated sites sees six sites at  $60^\circ$  azimuths. The locations are represented in Mercator projection in the main part of Figure 10.

It has appeared less than obvious to us that a global network of this size could conduct scheduled bistatic soundings (in a minimum cycle of six azimuths each) between pairs of stations without contention for the same observing period in the cycle.

Each sounder must select the appropriate transmit-receive antenna for the azimuth of its neighbor, without being required to serve another azimuth during the same period. The small numerals of Figure 10, at the midpoints of each station pair, suggest the extent to which this may be accomplished. Contention appears at six of the 260 midpoints (wherever the number of midpoints in a closed loop is odd), but otherwise an efficient and compatible schedule for bistatic and backscatter soundings seems attainable.

#### 4.2 The Geophysical Requirements

There are various ways of weighting the requirements for an ionospheric monitoring system, not the least important is that the system be realistic. Thus, we give weight to global monitoring of the F region with good fidelity while acknowledging that an equally faithful description of global sporadic E structures is probably unrealistic. For these we must be satisfied with the statistical data from regional sampling.

The correlation distance for foF<sub>2</sub> (noontime hourly data), for north-south and east-west directions, and for three seasons, is shown in Figure 11, from Rush and Edwards (1976). A 50% improvement of prediction of foF<sub>2</sub> at an unmeasured location, based upon data from a measured location, requires a correlation of 0.87 between the two locations (Gautier and Zacharisen, 1965). From Figure 11, station separations should lie in the range 1000-2000 km to achieve this. An improvement of prediction confidence can be accomplished at greater station separations, however, by increasing the correlation between them. We believe that this can be accomplished by estimating the local foF<sub>2</sub> gradient at each

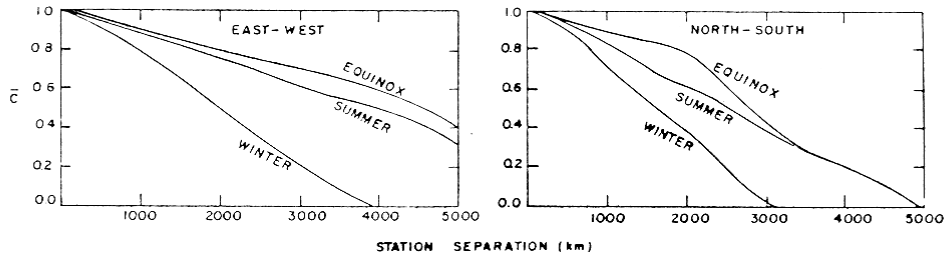


Figure 11. Correlation distance of foF2, noon values, from Rush and Edwards (1976), in longitude (left) and latitude (right) for three seasons.

location together with profile estimation at each midpoint.

Some recent results suggest a more definitive basis for deciding the geophysical requirements for station separation. Using AFA (Anharmonic Frequency Analysis; Paul, 1972), the temporal variations (diurnal and seasonal) of foF2 can be described by a small number of spectral components (Paul, 1978). About 9-11 spectral lines account for about 90% of the monthly median foF2 variation; they have a geographic variation that is more smooth than foF2 itself but still shows a strong dependence on solar activity. Figure 12 represents the latitude profile of the strongest component (the constant or zero-frequency average value) at two longitudes and two sunspot numbers. Figure 13 represents the second-strongest component (the 24-h diurnal line) at the two longitudes and for the same two levels of solar activity. The smallest spatial scales evident here are in the variation with latitude near the equatorial anomaly and are of the order of 10° of latitude or 1100 km. These features move in latitude, with sunspot number, a distance comparable to their width.

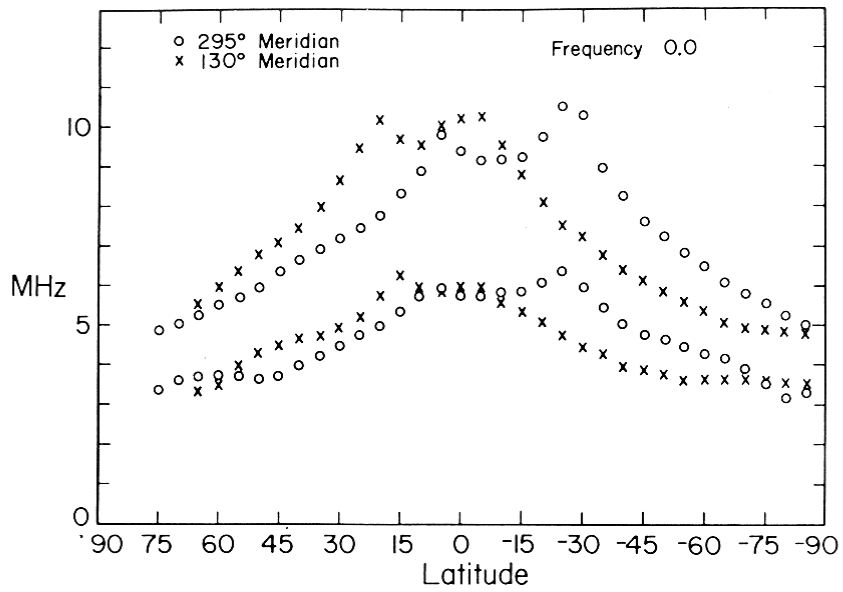


Figure 12. The constant component of foF2 from anharmonic frequency analysis (AFA) versus latitude along two meridians and at two levels of solar activity. SSN = 0, 100.

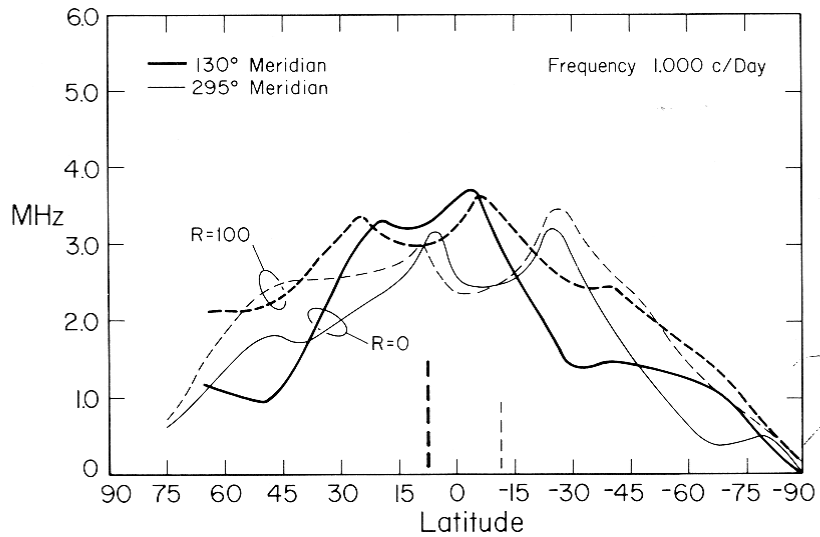


Figure 13. The diurnal component of foF2 from AFA at two levels of solar activity, along the 130° meridian.

The latitudinal gradient (dominated by the constant component, Figure 12) is about twice as large as the longitudinal gradient that is dominated by the diurnal variation (Figure 13), but the equatorial anomaly makes its own contribution to the longitudinal gradients in all components since the gradients depend upon whether the magnetic equator is north (longitude 130°) or south (295°) of the geographic equator.

We conclude that a station separation of about 2500 km in latitude is adequate for even the equatorial anomaly, assuming that bistatic sounding permits interpolation at the station midpoints, and that a somewhat larger separation is permissible in longitude except where the two equators are crossing at a steep angle (e.g., South America).

#### 4.3 New Standard Parameter Products From A Modern Network

Serious and difficult questions arise from the large information-gathering capability of the modern digital ionosonde, and the obvious problems may be compounded greatly in any large, coordinated network operation. The questions concern how much of the information to retain, where to archive it, and in what parametric form. A simplistic answer is to keep all of the raw data on magnetic tape and to maintain copies at the observing location (especially if it is itself a research or user's center) and at one or more World Data Centers. This answer can be defended for a transition period--and indefinitely, for certain events, locations, or world geophysical intervals--but it may have three unsatisfactory aspects as a general answer:



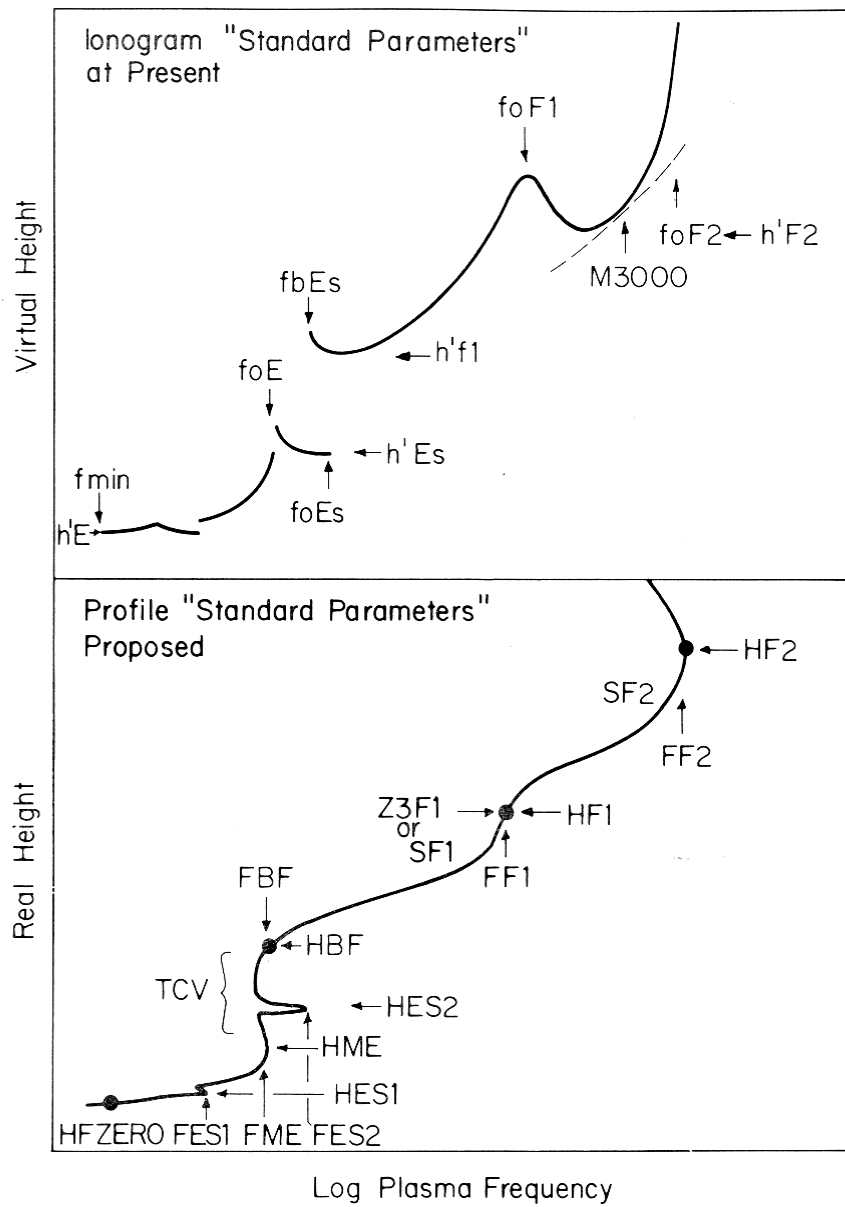


Figure 14. Top: The 11 standard parameters manually digitized from analog ionograms, exchanged internationally and archived in hourly tabulations at World Data Centers. Bottom: Some standard parameters that could serve to describe ionospheric electron density profiles and that could be summarized statistically.

- (1) The volume of raw information may be excessive; certain details plus statistical summaries may be sufficient.
- (2) The raw information is not in readily applicable form for geophysical or practical purposes.
- (3) Some reduction to geophysical units may be necessary in real time anyway, for efficiency of data acquisition. Automatic, adaptive real-time  $N(h)$  inversion is the principal example.

Currently ionosonde stations scale and data centers archive the 11 standard parameters from each hourly ionogram, which appear on the top panel of Figure 14. There are good and objective reasons to preserve the continuity of some of these parameters as long time-series at least for some locations (e.g., Washington) that got an early start. However, others of the standard parameters should be abandoned or redefined, for the reasons that they are subjectively defined (e.g., sporadic E types, foF1) or have indefinite meaning (M3000, h'F, f min). In the past, the subjectivity of manual ionogram scaling has helped to reduce the biasing effects of arbitrary rules in statistical summaries (at the price, of course, of artificial estimation noise that masks small but real fluctuations). There are some notable exceptions, however, where bias introduced by arbitrary definitions has dominated statistical summaries; for example, the incorrect estimation of foF2 near the auroral trough, the definition of foF1, and the treatment of spread F. Attempts to automate the definition of many of the present standard parameters

would surely introduce such biases and assumptions even more regularly.

We propose to initiate studies in a somewhat different direction, illustrated for  $N(h)$  profile data by the bottom panel of Figure 14. We assume that the profile has been obtained from virtual-height, frequency data at  $\lesssim$  frequencies that have been chosen adaptively by the ionosonde so that the desired detail is available in the profile. Virtual range measurements may also have been corrected for obliquity before inversion to  $N(h)$ . The figure defines a number of parameters with the following properties:

- (1) They characterize the profile sufficiently well that the profile itself can be reproduced from them to an acceptable accuracy.
- (2) They may each be summarized statistically into mean values and standard deviations (and possibly higher-order moments for suitable samples).
- (3) In their statistically-summarized form, they permit reversion to an acceptable mean profile. This procedure is analogous to that proposed by Dudeney (1978), except that in our case the parameters are literally properties of the  $N(z)$  profile; in his, Dudeney attempted to construct a profile using the old standard parameters plus a variety of assumptions.

The problem of reconstructing an average or instantaneous profile from these parameters that is an acceptable approximation to the true profile and that retains such desirable properties as differentiability need not be pursued here. It is already receiving considerable attention (Miller and Gibbs, 1980; Hill 1978), and we suggest only that the profile parameters proposed here could provide a better basis for such reconstructions.

A similar approach would be necessary for other kinds of information gathered by the system, for example,

- (1) Spaced-antenna complex-amplitude time series, converted to moving-pattern velocities and Doppler velocities, then summarized into vertical profile parameters:
  - Vx, Vy, Vz moving pattern velocity components at several (~10?) standard altitudes;
  - Vc, a random velocity or velocity standard deviation, at the same altitudes;
  - Vp, an ionization contour velocity.
- (2) A non-deviative absorption parameter from calibrated echo amplitude data on the underside E-region.
- (3) Deviative absorption parameters (or equivalent collision frequencies and/or temperatures) from echo-amplitude vs. group-path variations at HMAXF, HMAXF1, and HMAXE.
- (4) Variables describing the spectrum of electron density fluctuations. Scintillation parameters are easily

calculable (Wright, 1974) but their interpretation in terms of  $\Delta N/N$  and of irregularity scale is uncertain at present. On the other hand, in spread F,  $\Delta f/f$  gives  $\Delta N/N$  range of scales (Wright et al., 1977). Other estimates of  $\Delta N/N$  (with their scale) may accrue from controlled smoothing in least-squares profile inversion (Titheridge, 1978) and from echo obliquity measurements (Wright and Pitteway, 1979b, Figure 8). A central problem is to approach these several alternatives in an orderly way, so that a consistent and meaningful description of the observed irregularity spectrum is achieved.

Since it is already impossible to obtain long (e.g., 30-year) time series of the present standard parameters at most existing or suggested locations (except as we begin now, or recently, to obtain them), nothing is lost and much can be gained by redefinitions such as those proposed here. The old standard parameters can be continued at selected stations with existing long time series as a parallel effort until the spectral behavior (see §4.2) of the new parameters can be equated to (or distinguished from) the old.

#### 4.4 Volume of Information From a Modern Network.

The modern network will not yield an unmanageable volume of data. The weather services already cope with a much larger flow of data than that from our proposed network, and they are willing to see many of the raw measurements assimilated near their

sources into regional summaries of meaningful, diurnal parameters. A similar approach is worth consideration for a modern ionosonde network, with the supporting incentive that each system can provide the data-reduction facilities for most--if not all--of the measurements available locally and for the surrounding five or six cooperating systems. Each system is thus to be the center of its region, and it might archive locally more detail concerning its region than it shares. How large would the local and global data flows be?

#### 4.4.1 Data Volume From the Present Network.

First, let us see what is now, and what could be, obtained from the present network.

##### Analog ionogram accumulation:

- a) Four analog ionograms per hour, 8766 hours/year yield 35,000 ionograms/station.
- b) One hundred sixty stations yield  $5.6 \times 10^6$  ionograms/year.
- c) Assuming an average 100 stations, 1945-1980, we have accumulated about  $1.2 \times 10^8$  ionograms,
- d) At one station-month per film roll, we have 42,000 rolls of film.

##### Data now recovered by manual digitization (scaling):

- e) Hourly ionograms only, reduced to 11 parameters of, say, 1 byte (8-bits) each, yield  $9.6 \times 10^4$  bytes/station/year.
- f) One hundred sixty stations yield  $1.5 \times 10^7$  bytes/year.

- g) Since 1945, 100 stations have accumulated  $3.4 \times 10^8$  bytes.
- h)\* At 6250 BPI, one 9-track tape, with 80% data (20% record-gaps), has a capacity of  $1.6 \times 10^8$  bytes/tape. The global accumulation of scaled data requires 2.2 tapes.

Data potentially recoverable from analog films:

- i) Unassessed ionograms:  $10^3$  height boxes,  $10^3$  frequencies, 1 byte each, yield  $10^6$  bytes/ionogram;
- j) One hundred sixty stations yield  $5.6 \times 10^{12}$  bytes/year;
- k) Global accumulation since 1945 is  $2 \times 10^{14}$  bytes;
- l)\* If blindly put to tape, this requires  $1.2 \times 10^6$  tapes.
- m)\* Assessed echoes: say 1000 echoes/ionogram, 2 bytes each yield  $2 \times 10^3$  bytes/ionogram;
- n)\* One hundred sixty stations yield  $1.1 \times 10^{10}$  bytes/year, requires 70 tapes/year,
- o)\* Global accumulation of 100 stations, since 1945, requires 1531 tapes. This computer-accessible form is to be compared with 42,000 rolls of film.

4.4.2 Data Volume From a Modern Network

We assume some variant of B-Mode (Wright and Pitteway, 1979a) so that decimated ionograms (200 frequencies, at 6 times) are recorded each 10 minutes. Ninety-two observatories (Figure 9) add 260 bistatically-observed locations, for a total of 352 observing locations: We shall not distinguish, here, between

---

\*The data are not available in this form, but could be with effort.

what can be measured (or derived, or deduced) at vertical vs. oblique incidence.

At worst, if we were to retain everything:

- a) Unassessed recordings, 1000 range boxes, 200 frequencies, 6 times, 2 bytes (complex amplitude)  
=  $2.4 \times 10^6$  bytes/recording,
- b) At one recording each 10 minutes =  $3.5 \times 10^8$  bytes/day/station,
- c) With 352 locations =  $1.2 \times 10^{11}$  bytes/day,  
=  $4.4 \times 10^{13}$  bytes/year,  
= 280,000 tapes/year.

This is clearly prohibitive. Furthermore, in unassessed form, such raw data are of no use despite their retrievability.

Suppose a modernized set of standard parameters were devised, somewhat along the lines of §4.3, to summarize the height variations of electron density,  $\Delta N/N$ ,  $V_{x,y,z}$ , and, say 3 or 4 other parameters. We shall assume that the observed time dependence in B-mode (6 times) is assimilated into a smoothed representation at 5-min intervals, representing a factor of 2 increase of archived vs. observed instantaneous-time-dependent information.

We then have, as a proposed optimum the following volume of data:

- d) Forty ( $N(z) + \Delta N/N$ ) profile parameters, plus 3 velocity components each at 10 heights, plus 10 other parameters  
= 80 parameters/recording.



Multiplying by 2 for representation at intermediate times, 1 byte each, we get 160 bytes/10 minutes/location,

= 960 bytes/hour/location,

=  $8.4 \times 10^6$  bytes/year/location.

- e) Since 92 stations archive for 352 locations the yield would be  $3.2 \times 10^7$  bytes/year/station.
- f) With  $1.6 \times 10^8$  bytes/tape this requires 0.2 tapes/year/station local accumulation.
- g) Among the 92 stations the yield would equal 18 tapes globally, per year.

It is to be carefully noted that by this plan each of the 92 stations actually archives only its own vertical data and serves as the exclusive archive for several oblique paths; in other words, these numbers presume no duplicate archives. But in fact, it is desirable that each station archive data that describe the region around the station. Regions of three different sizes can be imagined:

- i) The circle, of about 1300-km radius, from each station to the midpoints of the oblique paths to the neighboring stations; or
- ii) The circle, of about 2600-km radius, to the neighboring stations; or
- iii) Total global sharing of all available data, at all stations.

In the extreme case (iii), each of the 92 stations would accumulate reduced data at the rate of 18 tapes/year, but this means, globally, 92 copies of the same information, and, while manageable, seems quite unnecessary. If the intermediate case (ii) is considered, we have five or six copies of this information (depending on the number of nearest stations), and this factor multiplies the conclusion of (f) above, so that only about one tape/year/station is required for regionally complete archives.

#### 4.5 Further Data Assimilation at Regional Centers.

The preceding discussion demonstrates the practicality of archiving a useful selection of the measurements at regional centers. What can then be done with them? There are many answers, dependent upon needs that are practicable because the data are geophysically meaningful and are in easily retrievable form. Figure 3 and §2.3 suggest some geophysical applications that might be pursued regularly or only occasionally at regional centers. We shall not attempt to assess the additional accumulations of deduced and derived information that could accrue in this way. Four further stages of assimilation will probably be desirable, however:

##### 4.5.1 Month by Hour Summaries.

Monthly-median values of some of the 11 standard parameters (Figure 14, top) are more widely available and used, at present, than the daily values from which they are obtained. They have proved satisfactory for long-range forecasts and for studies of

solar-cycle and seasonal dependencies. Including them with the archived data previously described obviously adds a negligible 3% to the data flow and to the archives. There is an unsatisfactory statistical aspect to the standard monthly medians however: the months are of uneven length, and as such, medians are only available after the end of the month. Better alternatives are obvious: mean values (rather than medians), standard deviations and higher moments (rather than quartile ranges), running windows (rather than calendar months). Furthermore, it might well be argued that with the basic data of §4.42 archived regionally, the statistical summaries need not be archived, but only recomputed as needed and then designed quite specifically for their intended application.

#### 4.5.2 Regional Mapping of Mean Values.

A good example of the conclusion to the preceding section is the production of regional maps representing the temporal summaries of deduced or derived parameters. Whether published (as numerical coefficients or geographically), or archived and computed only as needed, such maps have many obvious applications:

- possible reduction of data volume, accompanied by regional smoothing;
- interpolation, for the specification of ionospheric conditions at any location within the region;
- radio ray-tracing, for any radio path within the region;

- provision of a regional standard ionosphere that could, for example, be subtracted from instantaneous measurements to identify (and, on occasion, alert) the presence of significant events (e.g., those enumerated at the end of §2.4).

#### 4.5.3 Global Mapping of Mean Values.

Automated global mapping of median ionospheric characteristics (Rush and Edwards, 1976) is already a well-established process. However, the uneven distribution of stations (Figure 1), the uneven availability of parameters (§1.1), and the dependence on a rather heavy-handed mathematical procedure (Fourier analysis plus representation by spherical harmonics) have all multiplied to limit the diversity, economy, availability, and use of such maps. In a modern network, most of these limitations are removed or very broadly expanded, given only the necessary communications and computing facilities.

#### 4.5.4 Mapping of Spectral Components.

As a final refinement to the present standard procedures, we suggest that global mapping of the AFA spectral components of any of the available parameters be considered an ultimate goal. It has been shown (Paul, 1978, 1980) that the geographic variability of these spectral components (of foF2) is much more regular than the fully composed foF2. This will probably prove true for the proposed new parameters of Figure 14 (lower part), although, of course, it will take several years of observation and analysis before any spectral behavior can be established. To a limited

but still important extent, the older parameters might augment and improve the estimation of the spectral variations of the newer parameters, thus providing another important link between past and future methods. For example, the spectral variations of (foF2,FF2), (1/M3000,HF2), (foF1,FF1), (foE,FME), (foEs,FES), (h'E,HFZERO) might be identical or fairly simply related (in dimensionless amplitude and phase) even when the parameters of a pair are quite dissimilar.

#### 5.0 THE DEPLOYMENT OF A PRACTICAL MODERN NETWORK

Figure 15 (back cover) and the front cover provide global views of an optimum network of modern ionosonde instruments, based upon the requirements and technological opportunities reviewed above. At about 89 practical locations, we envision instruments capable of providing all of the detailed vertical incidence sounding information of the advanced digital ionosonde, plus additional information on lateral structure and gradients near each site, plus bistatic soundings between nearby pairs of sites.

Typical interstation distances in Figure 15 are about 2500 km, although many (e.g., Dublin-Prague) are less than 2000 km, and some, still useable for oblique soundings, are between 3000 and 4000 km (Seattle-Hawaii; Aricebo-Azores).

In the deployment of Figure 15, about 24 locations are "mandatory", since they are isolated islands whose absence would leave unnecessary and serious gaps in global coverage. A few such gaps are unavoidable anyway. Table 1 lists these with their

Table 1 - Gaps in Global Ionospheric Monitoring

| Present Network (Fig. 1)               | An Optimum Network (Fig. 15)          |
|--|---------------------------------------|
| S.Pacific Ocean<br>(8000 x 12000 km)   | S.Pacific Basin<br>(5500 x 9000 km)   |
| E.Equatorial Pacific<br>(8000 x 10000) | E.Equatorial Pacific<br>(5000 x 7000) |
| Indian Ocean<br>(6500 x 9000)          | S.Australian Basin<br>(4000 x 5000)   |
| S.Atlantic Ocean<br>(6500 x 6500)      | Mid Atlantic Basin<br>(4000 x 5000)   |
| N.Polar Cap<br>(2000 x 6000)           | N.W.Pacific Basin<br>(3500 x 5000)    |
| Africa<br>(4000 x 6000)                |                                       |
| S.America<br>(3000 x 6000)             |                                       |
| N.America<br>(2000 x 4000)             |                                       |

approximate dimensions (they are all oceanic), and lists, for comparison, the large gaps in the present network (Figure 1).

A list of the station locations of Figures 1 and 15 is given in Table 2. The 158 traditional stations, and 89 locations of the modern plan, have 41 places in common. Of the 24 mandatory island locations, five are currently instrumented. Eleven more of the 89 were once occupied by ionosondes and have become inactive. This overlap of the present network with our plan is intentional, reflecting our presumption that an existing station has a motivated administration behind it, experienced personnel, and a practical site. Stations marked "D" in our list are judged difficult logistically, but several of these (e.g., Pitcairn

Table 2. CURRENTLY ACTIVE IONOSONDE STATIONS AND A SUGGESTED OPTIMUM NETWORK

| Map Code | Present Stations         | Map Code | Suggested Stations      | Map Code | Present Stations       | Map Code | Suggested Stations           |
|----------|--------------------------|----------|-------------------------|----------|------------------------|----------|------------------------------|
| AB       | Aberystwyth (Wales)      |          |                         | CV       | Cape Zevgari (Cyprus)  |          |                              |
| AC       | Accra (Ghana)            |          |                         |          |                        | CA       | Carnarvon (Aust.)            |
|          |                          | AD       | Adak (U.S.A.) P,M       | CG       | Changhan (China)       |          |                              |
|          |                          | AL       | Adelaide (Aust.)        | GH       | Christchurch (N.Z.)    |          |                              |
| AH       | Ahmedabad (India)        |          |                         |          |                        | CD       | Chokurdakh (U.S.S.R.)        |
| AK       | Akita (Japan)            |          |                         |          |                        | XM       | Christmas Isl. (U.K.) P,D,M  |
| AA       | Alma Ata (U.S.S.R.)      |          |                         | CH       | Churchill (Can.)       | CH       | Churchill                    |
|          |                          | AN       | Angola                  |          |                        | CS       | Cocos Isl. (Aust.)           |
|          |                          | AK       | Ankara (Turkey)         |          |                        | CO       | College                      |
| AR       | Aricebo (U.S.A.)         | AR       | Aricebo                 | CO       | College (U.S.A.)       |          |                              |
| AI       | Argentine Isl. (U.K.)    | AI       | Argentine Isl. M        | CP       | Concepción (Chile)     | CP       | Concepción                   |
|          |                          | AE       | Ascension Isl. (U.K.) M | CG       | Chongqing (China)      |          |                              |
| AS       | Ashkabad (U.S.S.R.)      | AS       | Ashkabad                | DK       | Dakar (Senegal)        | DK       | Dakar                        |
| AT       | Athens (Gr.)             |          |                         |          |                        | DS       | Dar es Salaam (Tanz.)        |
| AU       | Auckland (N.Z.)          | AU       | Auckland                |          |                        | DW       | Darwin (Aust.)               |
|          |                          | AZ       | Azores (Port.) M        | DH       | Delhi (India)          | DH       | Delhi                        |
| BK       | Bangkok (Thai.)          | BK       | Bangkok                 | DT       | DeBilt (Neth.)         | DG       | Diego Garcia Isl. (U.K.) D,M |
| BB       | Baudouin (Belg.)         | BB       | Baudouin                | DI       | Dixon (U.S.S.R.)       |          |                              |
| BN       | Beiging (Peking) (China) |          |                         | DJ       | Djibouti (Fr.)         | DJ       | Djibouti                     |
| GE       | Belgrano (Argent.)       |          |                         | DB       | Dourbes (Fr.)          | DN       | Dublin (Ire.)                |
| BE       | Beograd (Yug.)           |          |                         | DU       | Dushanbe (U.S.S.R.)    |          |                              |
| BO       | Billerica (U.S.A.)       |          |                         |          |                        | EI       | Easter Isl. (Chile) D,M      |
|          |                          | BG       | Bogota (Col.)           |          |                        | FG       | Fiji (N.Z.) P,M              |
| BM       | Bombay                   |          |                         |          |                        | FA       | Fort Archambault (Chad)      |
| BC       | Boulder (U.S.A.)         | BC       | Boulder                 | FZ       | Forteleza (Braz.)      | FZ       | Forteleza                    |
|          |                          | BV       | Bouvet Isl. (Nor.) D,M  | FM       | Fort Monmouth (U.S.A.) |          |                              |
| BB       | Bribie Island (Aust.)    |          |                         | FR       | Freiburg (Ger.)        |          |                              |
| BR       | Brisbane (Aust.)         | BR       | Brisbane                |          |                        | GL       | Galapagos (Ecuad.) D,M       |
| BU       | Budapest (Hung.)         |          |                         | GY       | Garchy (Fr.)           |          |                              |
| BA       | Buenos Aires (Argent.)   | BA       | Buenos Aires            | GO       | Godhavn (Den.)         |          |                              |
| CU       | Calcutta (India)         |          |                         | GS       | Goose Bay (Can.)       |          |                              |
| CI       | Campbell Isl. (N.Z.)     |          |                         | GK       | Gorky (U.S.S.R.)       |          |                              |
| CB       | Canberra (Aust.)         |          |                         | GR       | Grahamstown (S.Af.)    |          |                              |
|          |                          | CN       | Canton (China)          | GZ       | Graz (Aust.)           |          |                              |
| CF       | Cape Parry (Can.)        |          |                         | GQ       | Guangzhon (China)      |          |                              |
| CE       | Cape Schmidt (U.S.S.R.)  |          |                         |          |                        | GM       | Guam Isl. (U.S.A.) P,M       |
|          |                          | CT       | Capetown (S.Af.)        | HB       | Halley Bay (U.K.)      | HB       | Halley Bay                   |

(Key: (P) = previously instrumented; (M) = mandatory location; (D) = difficult logistically).

Table 2. CURRENTLY ACTIVE IONOSONDE STATIONS AND A SUGGESTED OPTIMUM NETWORK (cont.)

| Map Code | Present Stations         | Map Code | Suggested Stations          | Map Code | Present Stations         | Map Code | Suggested Stations          |
|----------|--------------------------|----------|-----------------------------|----------|--------------------------|----------|-----------------------------|
| HA       | Haik'ou (China)          |          |                             | MM       | Mauritius M              |          |                             |
| HN       | Hanover (U.S.A.)         |          |                             | MW       | Mawson (Aust.)           | MP       | Merida (Mex.)               |
| HE       | Hermanus (S.Af.)         |          |                             | MX       | Mexico City (Mex.)       |          |                             |
| HS       | Highgate Springs (Aust.) |          |                             |          |                          | MY       | Midway (U.S.A.) M           |
| HO       | Hobart (Aust.)           |          |                             | MZ       | Miedzeszyn (U.S.S.R.)    |          |                             |
| HK       | Hong Kong (U.K.)         |          |                             | MH       | Millstone Hill (U.S.A.)  |          |                             |
| HU       | Huancayo (Peru)          |          |                             |          |                          | MQ       | Mindanao (Phillipines)      |
| IB       | Ibadan (Nig.)            | IB       | Ibadan                      |          |                          | MI       | Mirny                       |
|          |                          | HT       | Camp Heurtin (Fr.) D,M      |          |                          | MO       | Moscow                      |
|          |                          | IR       | Irkutsk                     | MI       | Mirny (U.S.S.R.)         |          |                             |
| IR       | Irkutsk (U.S.S.R.)       |          |                             | MO       | Moscow (U.S.S.R.)        |          |                             |
| IS       | Istanbul (Turk.)         |          |                             | MU       | Mundaring (Aust.)        |          |                             |
| JI       | Jicamarca (Peru)         | JI       | Jicamarca                   | MK       | Murmansk (U.S.S.R.)      | MC       | Muscat (Oman) D,M           |
| JO       | Johannesburg (S.Af.)     |          |                             |          |                          | NQ       | Narssarssuaq                |
| JR       | Juliusruh (Ger.)         |          |                             | NR       | Nairobi (Kenya)          |          |                             |
| KL       | Kaliningrad (U.S.S.R.)   | KG       | Kerguelen Isl. (Fr.) M      | NQ       | Narssarssuaq (Den.)      |          |                             |
| KR       | Karaganda (U.S.S.R.)     |          |                             | NI       | Norfolk Isl. (Aust.)     |          |                             |
| KB       | Khabarovsk (U.S.S.R.)    | KY       | Khaybar (Saudi Arabia)      | NO       | Norilsk (U.S.S.R.)       |          |                             |
|          |                          |          |                             | NR       | Novokazalinsk (U.S.S.R.) |          |                             |
| KV       | Kiev (U.S.S.R.)          |          |                             | NS       | Novosibirsk (U.S.S.R.)   |          |                             |
| KT       | Kiruna (Sw.)             |          |                             | NU       | Nurmijärvi (Fin.)        | OM       | Omsk (U.S.S.R.)             |
| KO       | Kodiakanal (India)       | KU       | Kourou (Fr.Guiana)          | OU       | Oagadougou (Fr.)         | PO       | Palermo, Sicily (It.)       |
|          |                          | KW       | Kwajalein Isl. (U.S.A.) P,M |          |                          |          |                             |
| LA       | Lancaster (U.K.)         | LC       | Lanchow (China) P           | PK       | Patrick AFB (U.S.A.)     |          |                             |
|          |                          |          |                             |          |                          |          |                             |
| LN       | Lannion (Fr.)            |          |                             |          |                          |          |                             |
| LZ       | Lanzhou (China)          | LP       | La Paz (Mex.)               | PA       | Point Arguello (U.S.A.)  |          |                             |
| LT       | Leicester (U.K.)         |          |                             | PT       | Poitiers (Fr.)           |          |                             |
| LD       | Leningrad (U.S.S.R.)     |          |                             |          |                          |          |                             |
| LI       | Lindau (Ger.)            | LB       | Lisbon (Port.)              | PS       | Port Stanley (U.K.)      | PQ       | Prague (Czech.)             |
| LY       | Lycksele (Sw.)           | MQ       | Macquarie Isl. (N.Z.) P,M   |          |                          | PS       | Port Stanley                |
|          |                          |          |                             |          |                          | PR       | Post Maurice Cartier (Alg.) |
| MD       | Madras (India)           |          |                             | RA       | Raratonga (N.Z.)         | RA       | Raratonga M                 |
| MG       | Magadan (U.S.S.R.)       | MG       | Magadan                     | RB       | Resolute Bay (Can.)      |          |                             |
| MN       | Manila (Phillipines)     |          |                             |          |                          | RJ       | Rio de Janeiro (Braz.)      |
|          |                          | MR       | Marion Isl. (S.Af.) P,M     | RO       | Rome (It.)               |          |                             |
|          |                          | MS       | Marquesas Isl. (Fr.) M      | RV       | Rostov (U.S.S.R.)        |          |                             |
|          |                          | MT       | Mato Grosso, (Braz.) D      | SH       | Sachs Harbor (Can.)      |          |                             |
| MA       | Maui (U.S.A.)            | MA       | Maui M                      |          |                          |          |                             |
| ML       | Manzhouli (China)        |          |                             |          |                          |          |                             |



Table 2. CURRENTLY ACTIVE IONOSONDE STATIONS AND A SUGGESTED OPTIMUM NETWORK (cont.)

| Map Code | Present Stations        | Map Code | Suggested Stations            | Map Code | Present Stations          | Map Code | Suggested Stations           |
|----------|-------------------------|----------|-------------------------------|----------|---------------------------|----------|------------------------------|
| SD       | Salerkhard (U.S.S.R.)   |          |                               | TH       | Thule (Den.)              | TH       | Thule                        |
| SY       | Salisbury (Rhod.)       | SY       | Salisbury                     | TC       | Thumba (India)            | TC       | Thumba                       |
| QM       | Sanae (S.Af.)           |          |                               | TI       | Tiruchchirappalli (India) |          |                              |
|          |                         | SA       | San Ambrosio Isl. (Chile) D,M | TX       | Tixie Bay (U.S.S.R.)      |          |                              |
| BZ       | San Jose (Braz.)        |          |                               | TO       | Tokyo (Jap.)              | TO       | Tokyo                        |
| SN       | San Juan (Arg.)         |          |                               | TK       | Tomsk (U.S.S.R.)          |          |                              |
| SB       | Scott Base (U.S.A.)     |          |                               | EB       | Portosa (Spain)           |          |                              |
| SM       | Søndrestrømfjord (Den.) |          |                               | TL       | Townesville (Aust.)       |          |                              |
|          |                         | SE       | Seattle (U.S.A.) P            | TW       | Trelew (Argent.)          | TT       | Tristan da Cunha (U.K.) D,M  |
| SU       | Seoul (Korea)           |          |                               | TR       | Trømsø (Nor.)             | TR       | Trømsø                       |
| SL       | Slough (U.K.)           |          |                               | TS       | Tsumeb (S.W.Af.)          |          |                              |
| SO       | Sodankylä (Fin.)        |          |                               | TU       | Tucuman (Argent.)         |          |                              |
| SQ       | Sofia (Bulg.)           |          |                               | TZ       | Tunguska (U.S.S.R.)       |          |                              |
| SG       | South Georgia (U.K.)    | SG       | South Georgia                 | UP       | Uppsala (Sw.)             |          |                              |
| ST       | South Uist (U.K.)       |          |                               | UA       | Ushaia (Arg.)             |          |                              |
| PO       | South Pole (U.S.A.)     |          |                               | VA       | Vanimo (New Guinea)       |          |                              |
|          |                         | BI       | Stanleyville (Bangui)         | VO       | Vostok (U.S.S.R.)         |          |                              |
| SV       | Sverdlovsk (U.S.S.R.)   |          |                               | WK       | Wakkanai (Jap.)           |          |                              |
| SW       | Syowa (Jap.)            | SW       | Syowa                         | WP       | Wallops Isl. (U.S.A.)     | WP       | Wallops Isl.                 |
| TT       | Tahiti (Fr.)            |          |                               | WS       | White Sands (U.S.A.)      |          |                              |
|          | Taipei (Taiw.)          | TT       | Taipei                        | WU       | Wuch'ang (China)          |          |                              |
| TG       | Tangerang (India)       | TG       | Tangerang                     | YA       | Yakutsk (U.S.S.R.)        |          |                              |
| TQ       | Tashkent (U.S.S.R.)     |          |                               | YG       | Yamagawa (Jap.)           |          |                              |
| TB       | Tbilisi (U.S.S.R.)      |          |                               |          |                           | SA       | Yuzhno Sakhalinsk (U.S.S.R.) |
| TA       | Terre Adelle (Fr.)      | TA       | Terre Adelle                  |          |                           |          |                              |

Island, Cocos Island) have once hosted an ionosonde. Many of our choices of location are arbitrary--and they are almost entirely so, within a 500-km radius of the nominal station site name, or about the radius of the station labels shown in Figure 15. However, a significant relocation of any one station in our plan must be accommodated by smaller relocations of adjacent stations, or perhaps by adding or deleting a location and thus improving or compromising regional coverage. There are numerous locations where stations could be added to improve local coverage. Typical additional locations (given those of Table 2, Figure 15) might be central France, western Egypt, western China, Mahi Island, Central Australia, Iceland. Where long time series of observations (e.g., Moscow, Washington) or a permanently important geophysical observatory (Aricebo, Tr msso, Jicamarca) compels a choice of location, freedom to select surrounding locations is further restricted. With these points clear, we should not wish our suggestion of optimum locations to express any deeper political considerations, and we hope that it is clearly understood that any rearrangement of locations that preserves approximately the suggested station density is equally satisfactory.

## 6.0 CONCLUSIONS

What steps are needed to bring about a plan of this kind? Setting aside practicalities temporarily, here are some significant technical problems worthy of study, approximately in order of decreasing priority:

- (1) The local-lateral-structure capabilities of the digital ionosonde require development and demonstration. The use of echolocation to describe tilts (with, or without, ray-tracing refinements) must be combined with existing programs for deducing the vertical structure (profile inversion). The methods should be tested against a satellite plasma probe; if the satellite is within a few scale heights of the (topside) F2 peak, then the local, horizontal log-gradient there should be equal to that at and near the peak.
- (2) A-mode, the adaptive, real-time  $N(z,t)$  capability of the Dynasonde (Figure 8), should be demonstrated.
- (3) The suitability of A-mode sampling frequencies (which will change dynamically, as the ionosphere itself changes) for defining other height- and time-dependent derivatives must be tested and demonstrated. Such derivatives are tilts, drifts, and  $\Delta N/N$ .
- (4) A sampling method for deducing drifts (Paul, unpublished) requires further tests against the well-tested Kinesonde mode, so that the lengthy time series and time-series analysis of the latter method are obviated.
- (5) With pairs of digital ionosondes, and preferably with at least a standard ionosonde at the midpoint, the oblique-incidence (BISTAT, BAKSCTR) modes of measure-

ment, and data reduction, need development and demonstration. This is a large subject, but fortunately there have been a number of vigorous efforts to develop the necessary data inversion methods (Croft, 1972; DuBroff et al., 1978; Nielson and Watt, 1972; Rao et al., 1976; Rao and Hoover, 1975; Smith, 1970; Tanaka, 1979).

Some of these studies (1-4) are essential to the research application of the new digital ionosondes individually and will be pursued at NOAA and elsewhere in the natural course of developing Dynasonde software. The oblique incidence capabilities of item 5 (and other items of lower priority such as OPRTUNE) present less scientific than technical interest and may require specific administrative encouragement as part of a determined intent to modernize an administration's ionospheric monitoring program.

Turning to practicalities, the main questions are costs for hardware, installation, and operations. The NOAA instrument (Figure 2) represents a hardware investment of about \$120,000. A commercial equivalent might cost twice that, but the system design and its capability are probably somewhat overelaborate, at least for, say, half the stations of our plan. That design was intended from the beginning to provide a test-bed for refinement of ionosonde methods. We believe that as microprocessors continue to decrease in cost, while approaching the larger minicomputers in speed, memory size, and processing capability, the cost

for the basic vertical-incidence instrument should be kept below \$100,000 in commercial or large-scale production.

It is evident from the foregoing that we differ categorically with the views held by some (e.g., Bibl and Reinisch, 1978) that "the most important requirement for a monitoring ionosonde is low cost, since only a dense network of sounders can produce a global picture of the ionosphere" and that "two sets of ionosondes are needed, one for research and one for monitoring purposes."

We must emphasize however that there is no need for absolute uniformity among the digital ionosonde instruments comprising our proposed network. Stations offering occasional or frequent research facilities (or an ionosonde research center, in the manner of incoherent scatter centers such as Arecibo) will of course need relatively elaborate systems. Very isolated stations (gap-fillers) will need only a minimal system, to which additional hardware could easily be interfaced temporarily if the station becomes central to a geophysical campaign. The minimal requirements for any instrument are easily stated:

- (1) Programmability, since we must assume, especially for modern instruments entering the network soon, that we really do not yet know the best way to make a given measurement or compute a wanted parameter; software programmability is our best insurance policy.
- (2) Synthesized and stable radio frequencies.

- (3) Digitization of all echo parameters, with adequate resolution.
- (4) Modularity, affording easy maintenance, long MTBF, and low cost.

Some particular comments are applicable to educational and government administrations that have become accustomed to the operation of their own ionosonde and would find that it is not needed in our plan:

- (1) Clearly an economy of radio sounding activity is desirable on grounds of efficient use of the radio spectrum and minimizing radio interference; these considerations alone may eventually make our network suggestions imperative.
- (2) National administrations in Europe realized at the beginning of large-scale space research that a proliferation of individual national centers could be a weakening policy, as compared with the cooperative establishment of ESRO. The same considerations prevail in the field of high-energy particle accelerators (Amaldi, 1979). A similar approach is worth consideration for ionospheric sounding centers.
- (3) Modern communications permit large numbers of widely separated users to enjoy the use of one central, large computing facility, almost as if it were theirs alone. This can apply as well in multiple access to an iono-

spheric sounding facility, to obtain the latest data or a summary, or to take active control of a share of the ionosonde's measurement potential. Surely these possibilities, incorporating the advanced measurement ability of the center itself, must outweigh present advantages of operating one's own analog ionosonde.

- (4) At an intermediate level we consider the educational institution which can fill a gap and can identify ionospheric research as an important specialization. To such institutions the modern ionosonde offers a small but complete data processing center, in addition to its primary sounding functions.

The most essential ingredient of our plan is again administrative, and as geophysicists rather than administrators we are unable to provide it. We refer to the planning, funding, and coordination required to bring about a network of the kind and capability described in this paper, on a global or regional scale in a reasonable time. Such a network is virtually certain to evolve eventually anyway, say within the next 20 years, because of the progressive obsolescence of present ionosondes and the continuing need for monitoring ionospheric weather. But we suggest that if a few national or multinational efforts (e.g., by NATO) were coordinated internationally by URSI, a regional demonstration network could be realized within five years. The merits of expanding or duplicating the demonstration network could then be readily assessed.

## REFERENCES

- Amaldi, U. (1979), Particle accelerators and scientific culture. CERN 79-06, CERN-European Organization for Nuclear Research, Geneva.
- Antoniadias, D. A. (1976), Determination of thermospheric quantities from simple ionospheric observations using numerical simulation. *J. Atmos. Terr. Phys.* 38, p. 187.
- Argo, P. E., and I. J. Rothmuller (1979), PROPHET, an application of propagation forecasting principles. In *Solar-Terrestrial Predictions Proceedings, I: Prediction Group Reports*. R. F. Donnelly, ed. U.S. Dept. of Commerce, NOAA/ERL, p.312.
- Barry, G. H., and R. B. Fenwick (1969), Oblique chirp sounding. In: *Oblique Ionospheric Radiowave Propagation*, AGARD Conf. Proc. #13, p. 487.
- Baulch, R. N. E., and E. C. Butcher (1978), Direction-of-arrival of radio waves reflected from the E region. *J. Atmos. Terr. Phys.* 40, p. 1235.
- Becker, W., and P. Stubbe (1963), Temperature variations in the F region during the last sunspot cycle. *Proc. Intern. Conf. of the Ionosphere*, Inst. of Physics and the Physical Society, London.
- Bibl, K., and B. W. Reinisch (1978), The universal digital ionosonde. *Radio Sci.* 13, p. 519.
- Broche, P. (1977), Propagation des ondes acoustico-acent gravitationnelles excitées par des explosions. *Ann. Geophys.* 33, p. 281.
- Brownlie, D. D., L. G. Dryburgh, and J. D. Whitehead (1973), Measurement of the velocity of waves in the ionosphere: a comparison of the ray theory approach and diffraction theory. *J. Atmos. Terr. Phys.* 35, p. 2147.
- Chernov, Yu. A. (1971), Backscatter ionospheric sounding, JPRS 54893, Svyaz Press, Moscow,
- Chuang, S. L., and K. C. Yeh (1977), A method for inverting oblique sounding data in the ionosphere. *Radio Sci.* 12, p. 135.
- Croft, T. A. (1972), Skywave backscatter: A means for observing our environment at great distances. *Rev. Geophys. Space Phys.* 10, p. 73.
- Danilkin, N. P., P. F. Denysenko, V. I. Vodolazkin, S. M. Sushchiy, and Y. U. N. Fayer (1978), Effective collision frequency in the E region of the ionosphere. *Geomag. Aeronomy* 18, p. 97.
- Davies, K. D. (1965), Ionospheric radio propagation. *Nat. Bur. Stds. Monograph 80*. Supt. Docs., Washington, D.C.
- DuBroff, R. E., N. N. Rao, and K. C. Yeh (1978), Backscatter ionogram inversion by ray-tracing methods. RADC-TR-78-86.




- Dudney, J. R., (1978), An improved model of the variation of electron concentration with height in the ionosphere. *J. Atmos. Terr. Phys.* 40, p. 195.
- Fedor (1967), A statistical approach to the determination of three-dimensional ionospheric drifts, *J. Geophys. Res.* 72, p. 5401.
- Ganguly, S. (1974), Estimation of electron collision frequency in the lower thermosphere. *J. Geophys. Res.* 79, p. 3235.
- Gautier, T. N., and D. H. Zacharisen (1965), Use of space and time correlation in short-term ionospheric predictions. Conf. Record, First Annual IEEE Communications Convention.
- Harper, R. M., and S. A. Bowhill (1974), Digital-ionosonde studies of F-region waves. U. Ill. Aeronomy Rep. No. 60.
- Hatfield, V. E. (1970), Derivation of ionospheric parameters from backscatter data. In: *Ionospheric Forecasting*, AGARD Conf. Proc. #49.
- Hatfield, V. E. (1979), HF communications predictions 1978 (An economical up-to-date computer code, AMBCOM). In *Solar-Terrestrial Predictions Proceedings, I: Prediction Group Reports*. R. F. Donnelly, ed., U.S. Dept. of Commerce, NOAA/ERL, p. D2-1.
- Hedin, A. E., H. G. Mays, C. A. Reber, N. W. Spencer, and G. R. Carignan (1972), Empirical model of global thermospheric temperature and composition based on data from the OGO-6 quadrupole mass spectrometer. NASA Goddard Space Flight Center Rep. X 621-73-37.
- Hill, J. R. (1978), Exact ray paths in a multisegment quasi parabolic ionosphere. NOSC Tech. Rep. 300, Naval Ocean Systems Center, San Diego, Calif.
- Marcos, F. A. (1966), Aircraft-induced ionospheric disturbances. *Air Force Surveys in Geophysics* No. 175, AFCRL (now AFGL).
- Miller, D. C., and J. Gibbs (1980), Analytic ray tracing techniques and applications to high frequency communication problems. RADC-TR-80-29 Final Tech. Rep.
- Morgan, M. G., H. J. Calderon, and K. A. Ballard (1978), Techniques for the study of TID's with multi-station rapid-run ionosondes. *Radio Sci.* 13, p. 729.
- Najita, K., P. F. Weaver, and P. C. Yuen (1974), A tsunami warning system using an ionospheric technique. *Proc. IEEE* 62, p. 563.
- Nielson, D. L., and T. M. Watt (1972), Ionospheric profile inversion using oblique-incidence ionograms. In: *Mathematics of Profile Inversion*, L. Colin, ed., NASA Tech. Memorandum TM X-62, 150, p. 4.
- Noxon, J. F., and A. E. Johanson (1972), Changes in thermospheric molecular oxygen abundance inferred from twilight 6300 Å airglow. *Planet. Space Sci.* 20, p. 2125.

- Paul, A. K. (1972), Anharmonic frequency analysis. *Math. Comput.* 26, p. 437.
- Paul, A. K. (1977), A simplified inversion procedure for calculating electron density profiles from ionograms for use with minicomputers. *Radio Sci.* 12, 119-122.
- Paul, A. K. (1978), Temporal and spatial distribution of the spectral components of foF2. *J. Atmos. Terr. Phys.* 40, 135-144.
- Paul, A. K. (1980), Proposal for mapping the spectral components of foF2. To be published as Proc. Workshop on Intern. Ref. Ionos.; UAG Report, World Data Center A, Boulder, Colo.
- Paul, A. K., G. H. Smith, and J. W. Wright (1968), Ray-tracing synthesis of ionogram observations of a large local disturbance in the ionosphere. *Radio Sci.* 3, p. 15.
- Paul, A. K., J. W. Wright, and L. S. Fedor (1974), The interpretation of ionospheric radio drift measurements--VI. Angle-of-arrival and group path (echolocation) measurements from digitized ionospheric soundings: The group path vector. *J. Atmos. Terr. Phys.* 36, p. 193.
- Pfister, W. (1971), The wave-like nature of inhomogeneities in the E-region. *J. Atmos. Terr. Phys.* 33, p. 999.
- Prölss, G. W., K. H. Fricke, and U. von Zahn (1975), Observations during a magnetic storm in late October, 1973. *Space Research XV*, M. J. Rycroft, ed. Akademie-Verlag, Berlin, p.215.
- Rao, N. N., and K. E. Hoover (1975), Derivation of ionospheric layer parameters from angles of arrival of HF radio waves. *J. Atmos. Terr. Phys.* 37, p. 1167.
- Rao, N. N., K. C. Yeh, M. Y. Youakim, K. E. Hoover, P. Parhami, and R. E. DuBroff (1976), Techniques for determining ionospheric structure from oblique radio propagation measurements. RADC-TR-76-401.
- Rishbeth, H., and O. K. Garriott (1969), Introduction to ionospheric physics. Academic Press, New York and London.
- Rishbeth, H., and H. Kohl (1976), Topical questions of ionospheric physics: A working group report. *J. Atmos. Terr. Phys.* 38, p. 775.
- Rohrbaugh, J. L., W. E. Swartz, and J. S. Nisbet (1973), Comparison of incoherent scatter and ionosonde measurements of temperature with calcium plage and 2800 MHz intensities. *J. Geophys. Res.* 78, p. 281.
- Rush, C. M. (1976), An ionospheric observation network for use in short-term propagation predictions. *Telecom. J.* 43, p. 544.
- Rush, C. M., and W. R. Edwards, Jr. (1976), An automated mapping technique for representing the hourly behavior of the ionosphere. *Radio Sci.* 11, p. 931.

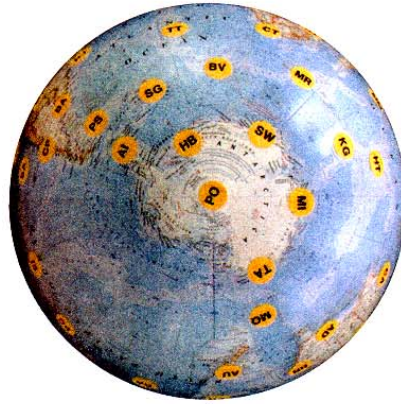
- Ruster, R. (1965), Ionospheric parameters during two successive polar magnetic substorms. *J. Atmos. Terr. Phys.* 27, p. 1229.
- Saha, A. J., and R. Venkatachari (1975), On extraction of collision frequency and temperature in F layer from absorption measurements. *Ind. J. of Radio and Space Phys.* 4, p. 310.
- Smith, M. S. (1970), The calculation of ionosphere profiles from data given on oblique incidence ionograms. *J. Atmos. Terr. Phys.* 32, p. 1047.
- Stubbe, P. (1973), Atmospheric parameters from ionospheric measurements. *Z. f. Geophys.* 39, p. 1043.
- Tanaka, T. (1979), Skywave backscatter observations of sporadic E over Japan. *J. Atmos. Terr. Phys.* 41, p. 203.
- Thome, G. (1964), Incoherent scatter observations of traveling ionospheric disturbances. *J. Geophys. Res.* 69, p. 4047.
- Thomson, R. L., and J. A. Secan (1979), Geophysical forecasting at AFGWC. In: *Solar-Terrestrial Predictions Proceedings, I: Prediction Group Reports.* R. F. Donnelly, ed. U.S. Department of Commerce, NOAA/ERL, p. 350.
- Titheridge, J. E. (1978), The generalized polynomial analysis of ionograms. Tech. Rep. 78/1a, Radio Research Center, Univ. Auckland, N.Z.
- UAG-54 (1976), Catalog of ionospheric vertical sounding data. World Data Center A, Solar-Terr. Physics, NOAA, Boulder, Colo.
- Vidal-Madjar, D., F. Bertin, and J. Testud (1978), Sur le jet-stream de la tropopause en tant que source des ondes de gravité observée dans la thermosphere. *Ann. Geophys.* 34, p. 1.
- Wright, J. W. (1963), Temperature control of the structure and variations of the quiet ionosphere. Proc. Internat. Conf. on the Ionosphere, Imperial College, London, July 1962. Publ. Inst. Phys. and the Physical Society, London.
- Wright, J. W. (1964), On the implication of diurnal, seasonal and geographical variations in compositions of the high atmosphere, from F-region measurements. Proc. NATO Adv. Study Inst., Electron Density Distribution in Ionosphere and Exosphere. North Holland Publishing Co., Amsterdam.
- Wright, J. W. (1969), Some current developments in radio systems for sounding ionospheric structure and motions. Proc. IEEE 57, p. 481.
- Wright, J. W., A. R. Laird, D. Obitts, E. J. Violette, and D. McKinnis (1972), Automatic N(z,t) profiles of the ionosphere with a digital ionosonde, *Radio Sci.* 7, p. 1033.
- Wright, J. W. (1974), Kinesonde studies of cesium ion clouds in the E-region. In: *Methods of measurements and results of lower ionosphere structure*, K. Rawer, ed. COSPAR Symposium, Akademie-Verlag, Berlin.

- Wright, J. W. (1975a), Development of systems for remote sensing of ionospheric structure and dynamics: functional characteristics and applications of the "Dynasonde". NOAA ERL SEL 206, U. S. Dept. of Commerce, NOAA/ERL.
- Wright, J. W. (1975b), Evidence for precipitation of energetic particles by ionospheric "heating" transmissions. J. Geophys. Res. 80, p. 4383.
- Wright, J. W. (1977), Development of systems for remote sensing of ionospheric structure and dynamics: The Dynasonde data acquisition and dynamic display system. Special Rep., U.S. Department of Commerce, NOAA/ERL.
- Wright, J. W., and G. H. Smith (1967), Review of current methods for obtaining electron density profiles from ionograms. Radio Sci. 2, p. 1119.
- Wright, J. W., and M. L. V. Pitteway (1979a), Real-time data acquisition and interpretation capabilities of the Dynasonde. 1. Data acquisition and real-time display. Radio Sci. 14, p. 815.
- Wright, J. W., and M. L. V. Pitteway (1979b), Real-time data acquisition and interpretation capabilities of the Dynasonde. 2. Determination of magnetoionic mode and echolocation using a small spaced receiving array. Radio Sci. 14, p. 827.
- Wright, J. W., M. Glass, and A. Spizzichino (1975a), The interpretation of ionospheric radio drift measurements--VIII. Direct comparisons of meteor radar winds and kinesonde measurements: Mean and random motions. J. Atmos. Terr. Phys. 38, p. 21.
- Wright, J. W., G. Vasseur, and P. Amayenc (1975b), Direct comparisons between field-aligned ion drifts by incoherent scatter and kinesonde spaced-antenna measurements. J. Atmos. Terr. Phys. 38, p. 731.
- Wright, J. W., J. P. McClure, and W. B. Hanson (1977), Comparisons of ionogram and OGO-6 satellite observations of small-scale F region inhomogeneities. J. Geophys. Res. 82, p. 548.

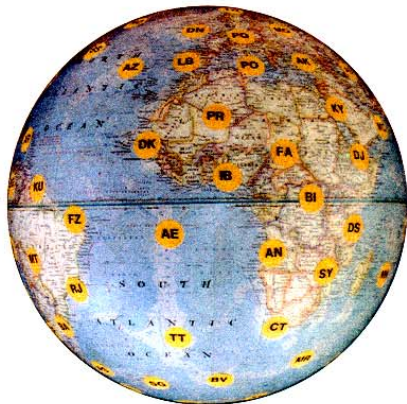
Figure 15. Suggested deployment of an optimum network, of about 90 modern digital ionosondes, also listed in Table 2. Each station would maintain an accurate three-dimensional local model applicable to a vertical cone of about the label radius, 500 km, at the F2 peak. Backscatter, bistatic oblique sounding, and other methods would maintain observations at about 250 intermediate locations. 



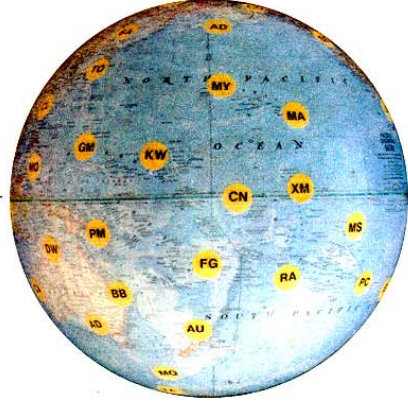
North Pole



South Pole



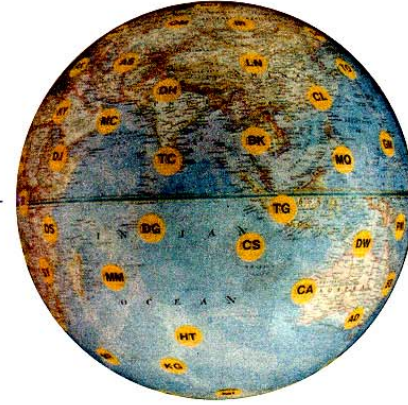
0°



180°



90° W



90° E